

**Hydraulic Tomography and High-Resolution Slug Testing to Determine  
Hydraulic Conductivity Distributions – Year 2**

The University of Kansas  
Department of Geology

Brett R. Engard  
Carl D. McElwee  
Rick Devlin  
Brian Wachter  
Benjamin Ramaker

Annual Report  
SERDP  
Strategic Environmental Research and Development Program  
Project # ER1367  
December 2006

VIEWS, OPINIONS, AND/OR FINDINGS CONTAINED IN THIS REPORT ARE  
THOSE OF THE AUTHORS AND SHOULD NOT BE CONSTRUED AS AN  
OFFICIAL DEPARTMENT OF THE ARMY POSITION, OR DECISION UNLESS SO  
DESIGNATED BY OTHER OFFICIAL DOCUMENTATION

## Table of Contents

<b>Background .....</b>	<b>3</b>
<b>Objective .....</b>	<b>3</b>
<b>Technical Approach .....</b>	<b>3</b>
<b>Introduction .....</b>	<b>4</b>
<b>Theory .....</b>	<b>13</b>
<b>Methodology</b>	
<b>Field Techniques .....</b>	<b>20</b>
<b>Data Processing .....</b>	<b>25</b>
<b>Results From High Resolution Slug Testing and     Continuous Pulse Testing .....</b>	<b>27</b>
<b>Calculation of “Anomalous K Values” .....</b>	<b>43</b>
<b>Reproducibility and Reciprocity .....</b>	<b>48</b>
<b>Diagonal Ray Path Data .....</b>	<b>49</b>
<b>Summary and Conclusions .....</b>	<b>51</b>
<b>References .....</b>	<b>54</b>
<b>Appendix</b>	
<b>A. Technical Publications .....</b>	<b>57</b>

**Background:**

A considerable body of research has shown that the major control on the transport and fate of a pollutant as it moves through an aquifer is the spatial distribution of hydraulic conductivity. Although chemical and microbial processes clearly play important roles, their influence cannot fully be understood without a detailed knowledge of the subsurface variations in hydraulic conductivity at a site. A number of theories have been developed to quantify, in a generic sense, the influence of these variations using stochastic processes or fractal representations. It is becoming increasingly apparent, however, that site-specific features of the hydraulic conductivity distribution (such as high conductivity zones) need to be quantified in order to reliably predict contaminant movement. Conventional hydraulic field techniques only provide information of a highly averaged nature or information restricted to the immediate vicinity of the test well. Therefore, development of new innovative methods to delineate the detailed hydraulic conductivity distribution at a given site should be a very high priority. The research proposed here is directed at addressing this problem by developing techniques with the ability to map 3-D hydraulic conductivity distributions.

**Objective:**

Since spatial changes in hydraulic conductivity are a major factor governing the transport and fate of a pollutant as it moves through an aquifer, we have focused on the development of new innovative methods to delineate these spatial changes. The objective of the research proposed here is to build on our previous research to develop and improve field techniques for better definition of the three-dimensional spatial distribution of hydraulic conductivity by using hydraulic tomography coupled with high-resolution slug testing.

**Technology Approach:**

We have been working for a number of years to quantify hydraulic conductivity fields in heterogeneous aquifers. One method we have worked on extensively that shows great promise is high-resolution slug testing. This method allows the delineation of the vertical distribution of hydraulic conductivity near an observation well. We propose to combine this method with another innovative method for investigating the hydraulic conductivity distribution between wells, called hydraulic tomography. We will use an oscillating signal and measure its phase and amplitude through space in order to estimate the hydraulic conductivity distribution of the material through which it has traveled. Our preliminary work has shown that the phase and amplitude of the received signal can be measured over reasonable distances. The high-resolution slug testing results will be used as an initial condition and will provide conditioning for the tomographic inverse procedure, to help with any non-uniqueness problems. Slug test data are most accurate near the tested well and should probably not be extrapolated blindly between wells. Together, slug testing and hydraulic tomography should be more powerful than either one used in isolation and should give the best opportunity to characterize the hydraulic conductivity in-situ by a direct measure of water flow, as an alternative to indirect methods using geophysical techniques.

## Introduction

A typical method used to determine fluid behavior in a geologic matrix near a well is a pumping test. Here a pump is installed into a well and groundwater is removed or injected while water levels in surrounding observation wells are monitored. Then the parameters mentioned above can be estimated by monitoring changes in water levels at observation wells at some distance. These types of tests are typically large in scale, (Schad and Teutsch, 1994). Another test is an interference test, which is a special pumping test where the pump discharge has a variable rate. Interference tests are conducted by variable production or injection fluid (hydraulic head changes) at one well, and observing the changing pressure or hydraulic head with time and distance at other locations. These tests are valued to estimate flow characteristics *in situ*, but are measures of the aquifer material over large volumes also.

On the other hand, physical cores of aquifer material can be obtained by a variety of drilling methods. These samples can then be tested in a laboratory (ie. falling or constant head permeability tests) to estimate the hydraulic properties. One advantage to this method is that the sample can be visually inspected. Some disadvantages to this method are that the material is disturbed from its natural environment and the sample is a small representation of the total aquifer.

Another common technique for determining aquifer parameters is to conduct slug tests. A slug test is the addition or extraction of a known volume of fluid to a well while monitoring the response of the aquifer material in order to estimate K. Slug testing is usually only conducted in a single well. It is generally accepted that the radius of influence of a slug test is small and only provides a limited view of subsurface

hydrogeologic properties near the well. Traditionally, slug tests have been initiated with the addition into a well of a known volume of water or a physical slug. More recently, pneumatic methods have become popular (Zemansky and McElwee, 2005; Sellwood, 2001; McCall et al., 2000) for multilevel slug testing. Slug tests in low K formations can take very much longer than in material with high permeability. To overcome this, the fluid column in a well can be pressurized and the pressure change with time can be used as an alternative (Bredehoeft and Papadopolos, 1980).

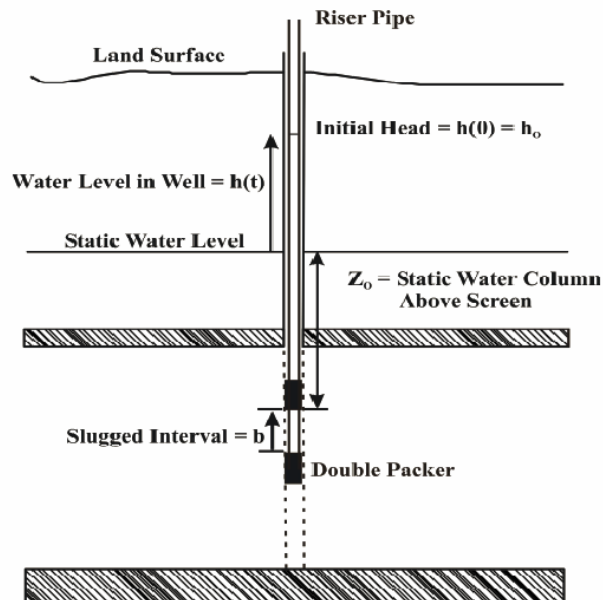


Figure 1. High resolution slug testing equipment deployed in a fully penetrating well.

Typical slug tests are conducted by exciting the entire length of the well screen. Whole well slug testing can provide information near the tested well but it is averaged over the total length of that well's screen. However, aquifers are naturally heterogeneous and whole well slug testing is unable to distinguish areas of high or low K. High resolution slug testing [(HRST), over short screen intervals (Figure. 1)] was developed to provide a more detailed vertical profile of K near the tested well. In this research the

HRST interval is approximately 0.5 m; but, stressed intervals as small as 5 cm have been used (Healey et al., 2004). Currently there is no accepted method to bridge the gap between the larger lateral well-to-well averages from pumping or interference tests and detailed vertical estimates of K from HRST. Proposed here is a method to obtain estimates of aquifer parameters at larger radii of influence, while simultaneously maintaining a higher resolution.

Pulse testing is one method of determining fluid flow parameters that is often employed by the petroleum industry. Johnson et al. (1966) published results to experiments conducted in a sandstone reservoir near Chandler, OK. It was found that the new pulse method was as effective as typical interference tests. The transient pressure signal is propagated by *in situ* fluid and is therefore a direct measure of reservoir diffusivity. Other advantages of the pulse method are the ability to distinguish the test from background noise because of its controlled frequency of oscillation and the reduction of down time relative to production. Since 1966, pulse testing has been used to delineate fractures (Barker, 1988; Brauchler, et al., 2001) and to predict water flood performance (Pierce, 1977).

The changes in groundwater levels as a result of tidal fluctuations have been well studied (Ferris, 1951) and (Jiao and Tang, 1999). The sinusoidal tidal fluctuations propagated inland through an aquifer are related to aquifer storativity and transmissivity. Solutions to water level fluctuations induced by seismic waves were presented by Cooper et al. (1965). The pressure head fluctuations controlling water levels are a result of the vertical motion of the aquifer but are dominated by dilation of the aquifer porosity. An interference test of alternating oil production and shut in time was conducted to

determine the interconnectivity of wells in a production field (Johnson et al., 1966). Here the source well is assumed to be a line source in an infinite homogeneous reservoir. The time lag and the received amplitude were used to estimate the average well-to-well transmissivity and storage properties of the reservoir. These oil field methods were theoretically adapted to hydrogeologic characterization by Black and Kipp (1981). Analytical solutions of a fracture responding to a single pulse interference test, a slug of water, was modeled and tested by Novakowski (1989). Straddle packers isolated the fracture and were used to apply the slug of water by being deflated. The duration of these tests was on average 30 min. The sequential pumping or removal of water was used to collect head responses between wells (Yeh and Liu, 2000). In these experiments multiple ray paths were analyzed as a hydraulic tomography experiment. Such experiments show promise in their ability to distinguish lateral and vertical 2-D variations in heterogeneity by changes in the signal over the travel path.

The research presented here uses continuous, controlled, sinusoidal pressure signals [the continuous pulse test (CPT)] as a means to estimate vertical profiles of well-to-well averaged hydraulic diffusivity. In this research, the primary method of stimulation of the alluvial aquifer was achieved by pneumatic methods. The column of air within a well was pressurized via an air compressor. A signal generator was used to open and close valves at the well-head allowing air to enter or exit the well. The signal generator produced an adjustable frequency step function, controlling the periodicity of the pulse-testing event. Theoretically, a square wave pressure test is the simplest to conduct because of the instantaneous pressure changes (Lee, 1982). Due to the input air pressure, the water column in a well will be depressed creating flow through the well

screen. This pulse of hydraulic pressure is transferred to the aquifer system based on the diffusivity of the material. As the air column within the well is allowed to return to atmospheric pressure, water will rush back into the well from the aquifer. These fluctuations are periodic and similar to tidal fluctuations acting upon a coastal aquifer system. The governing equations for an aquifer responding to tidal fluctuations were adapted to Cartesian, cylindrical, and spherical coordinate systems describing groundwater flow with sinusoidal boundary conditions.

The period, the phase, and the amplitude of the produced wave can then be measured simultaneously at the source well and at observation wells. Through dispersion, the aquifer material will decrease the fidelity of a step input, retard the propagation, and attenuate the propagating wave front, resulting in a phase lag or shift, and a decrease in the amplitude. The amplitude ratio [received amplitude  $A_r$  divided by the initial amplitude  $A_0$ ] and the phase difference [reference phase  $\phi_0$  minus the received phase  $\phi_r$ ] can then be used to calculate the hydraulic diffusivity (Lee, 1982).

Zero Offset Profile (ZOP, source and receiver at same elevation) CPT data and Multiple Offset Gather (MOG, source location fixed receiver elevation varied) CPT data were collected at the University of Kansas' Geohydrologic Experimental and Monitoring Site, (GEMS) a well-studied shallow semi-confined alluvial aquifer system in the Kansas River floodplain. Line sources equal to the total screen length and point sources isolated by custom bladder packers were used in these experiments. Field data indicate that sinusoidal signals can propagate reasonable distances, and may provide estimates of the well-to-well diffusivity. Vertical profiles of hydraulic conductivity ( $K$ ), measured with high-resolution slug testing (HRST) were collected for correlation with the CPT data.



The study area is the University of Kansas GEMS area located in Douglas County, northeast Kansas, along the northern margin of the Kansas River flood plain (Figure. 2). GEMS is in a Pennsylvanian bedrock valley filled with Wisconsin-age glaciofluvial terrace sediments (Schulmeister, 2000). The upper 11 m of sediments are mostly silts and clays and the lower 12 m of sediments at GEMS consists of a fining upward sequence of pebbles, coarse sand, and fine sand, which is underlain by the Tonganoxie Sandstone (Jiang, 1991). Within the sequences of sandy material are lenses of low permeability fine-grained sediments. These clay lenses occur at various elevations and can be up to 1 m thick (Schulmeister, 2000 and Healey et al., 2004). As an aquifer, the Kansas River alluvium is a prolific deposit of unconsolidated sands and gravels. It is a high yielding semi-confined aquifer meeting the needs of agricultural, industrial, and community interests.

Many studies have been conducted at GEMS and many well nests have been completed to various depths with various screen lengths. Porosity, grain size, and laboratory K calculations were performed by collecting physical samples of the aquifer material (Jiang, 1991). A single well injection tracer test was used to estimate a K distribution by monitoring the transport of an electrolytic solution (Huettl, 1992). The K distribution in an area of GEMS was also estimated by conducting an induced-gradient tracer test through a multilevel groundwater sampling well field (Bohling, 1999). Direct push bulk electrical conductivity (EC) profiling (Figure 3) and direct push pneumatic slug tests were also done adjacent to the tracer experiment well field (Sellwood, 2001).

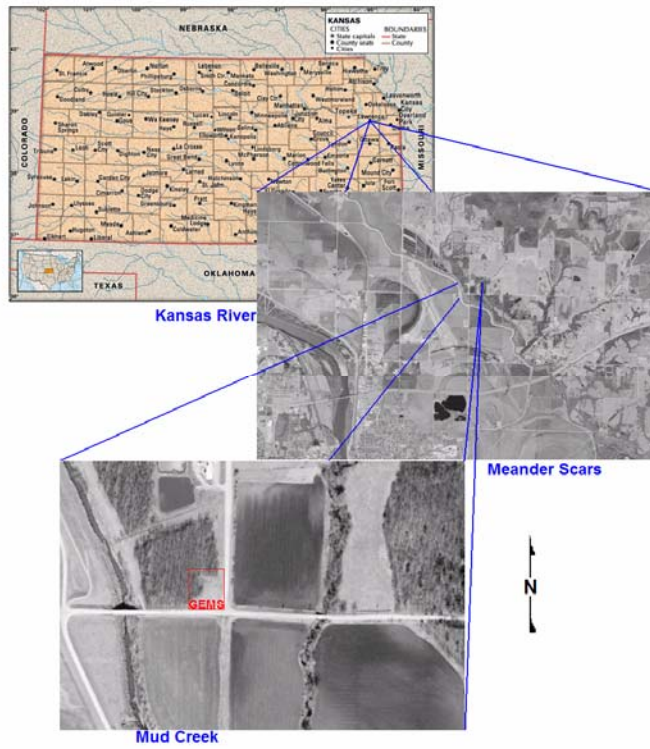


Figure 2. GEMS location map and aerial photographs.

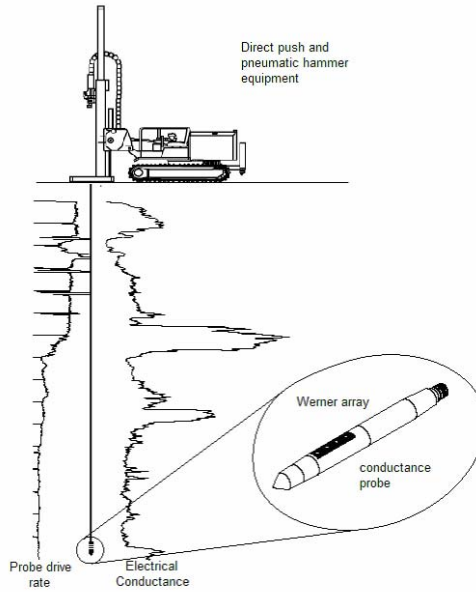


Figure 3. Direct push drilling unit, Electrical Conductance probe, and example profile.

Most recently, HRST K estimates were collected in numerous wells, which were fully screened through the aquifer material (Ross, 2004). The monitoring well locations used in this project are shown in Figures 4. Table 1 lists some information about wells used in this research. These independent studies and the research presented here all produced estimates of K that can be collected into a database. After compiling this data, vertical and lateral variations of the K distribution are evident. Typically at GEMS, K increases with depth in the sands and gravels, and low K material can be associated with high EC measurements. In some areas at the GEMS, “layers” or zones of high K material are apparent. The high EC readings are also often laterally continuous.

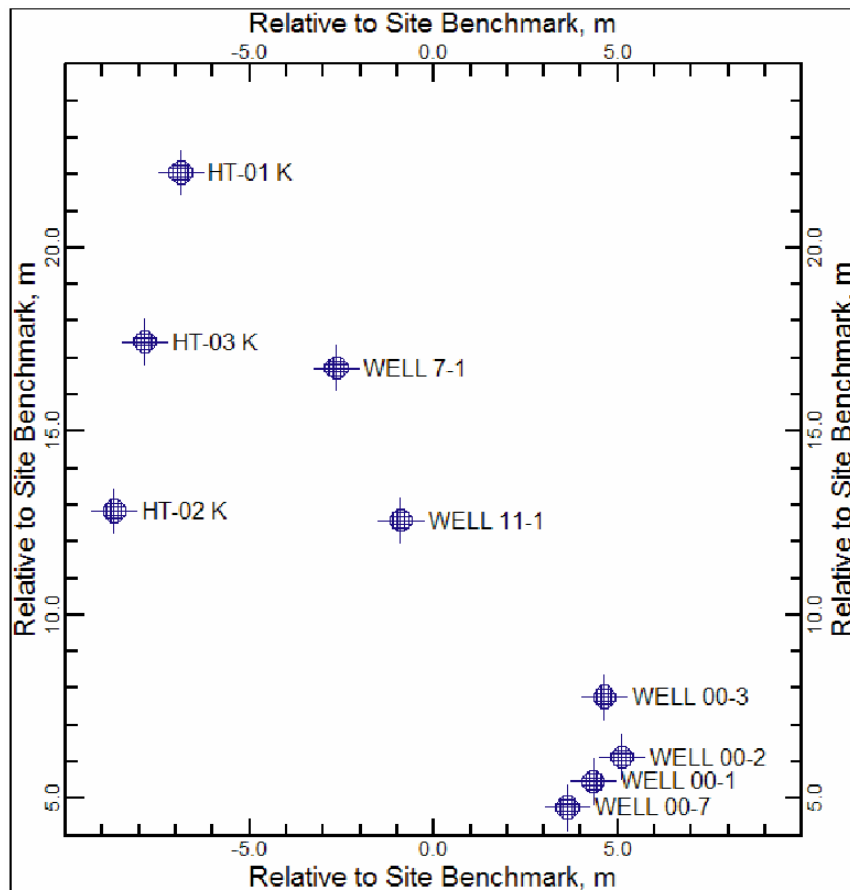


Figure 4 Map of GEMS wells used in this research project

**Table 1. Well Information**

Location	Elevation ft	Elevation m	Depth ft	Depth m	Screen ft	Screen m
Corps Stake	827.556	252.304	-----	-----	-----	-----
HT-1	829.946	253.032	73.290	22.345	30.0	9.14
HT-2	829.576	252.920	72.670	22.155	30.0	9.14
HT-3	829.000	252.744	69.000	21.037	30.0	9.14
7-1	828.416	252.480	68.850	20.991	30.0	9.14
11-1	828.306	252.532	64.400	19.634	45.0	13.72
00-1	828.823	252.690	55.900	17.043	2.5	0.762
00-2	829.115	252.779	14.410	4.393	2.5	0.762
00-3	828.774	252.675	70.370	21.454	30.0	9.14
00-7	828.958	252.731	66.730	20.345	2.5	9.14

**Well to Well Radial Distances, r**

Well	to Well	Distance, r m
00-3	00-2	1.52
	00-1	2.32
	00-7	3.62
	11-1	7.26
	7-1	11.5

Well	to Well	Distance, r m
7-1	11-1	4.51
	HT-3	5.14
	HT-1	6.44
	HT-2	6.91

Well	to Well	Distance, r m
HT-2	HT-3	4.36

Well	to Well	Distance, r m
HT-1	HT-3	4.76
	HT-2	9.13

## Theory

Fluid flow in saturated aquifers behaves much like heat flow and can be described by similar equations. Excess pore pressures, matrix permeability, compressibility, and storativity all influence the fluctuations of groundwater levels in response to applied stresses. The excess fluid pressure  $P_e$ , above hydrostatic pressure  $P_s$ , is related to the total stress on the aquifer  $\sigma$ , and changes the stress  $\Delta\sigma$  by

$$(1) \quad \sigma + \Delta\sigma = \sigma_e + (P_s + P_e)$$

The above equation allocates the additional stress to either the aquifer matrix itself or to excess hydraulic pressure,  $P_e$ . By changing the hydraulic pressure or hydraulic head, the water levels in an aquifer will also change accordingly. The total hydraulic head ( $h$ ) hydraulic potential measured in a well is a combination of the elevation head  $z$ , and the hydraulic pressure head  $P$

$$(2) \quad h = z + P/\rho g$$

such that

$$(3) \quad P = P_s + P_e$$

Since the elevation is static, the only dynamic portion of  $h$  is due to pressure changes as shown in the following equation

$$(4) \quad \frac{\partial h}{\partial t} = \frac{1}{\rho g} \frac{\partial P}{\partial t}$$

where  $\rho$  is the fluid density and  $g$  is the acceleration of gravity. Substituting equation (3) into equation (9) the total head measured in a well can also be expressed as

$$(5) \quad h = z + (P_s/\rho_w g + P_e/\rho_w g)$$

Darcy's law states that the discharge  $Q$  of a fluid through a porous media depends on the hydraulic gradient (the change in head with distance)  $\frac{\partial h}{\partial L}$ , and the cross sectional area  $A$ .

Darcy's Law is

$$(6) \quad Q = -KA \frac{\partial h}{\partial L} .$$

Darcy's proportionality constant  $K$ , now called hydraulic conductivity, is a measure of how easily a fluid will flow through an aquifer. By combining equation (5) with equation (6) the one-dimensional horizontal flow in the  $x$  direction  $q_x$  is

$$(7) \quad q_x = -K_x \left( \frac{\partial h}{\partial x} \right) = -K_x \left( \frac{\partial}{\partial x} \right) \left[ z + \left( \frac{P_s}{\rho g} + \frac{P_e}{\rho g} \right) \right]$$

Assuming that  $z$  and  $P_s$  are constant, the flow due to excess pressure is

$$(8) \quad q_x = -\frac{K_x}{\rho g} \left( \frac{\partial P_e}{\partial x} \right)$$

Diffusivity is the ratio

$$(9) \quad D = T/S = K/S_s.$$

$D$  is a measure of the ability of an aquifer to transmit changes in the hydraulic head. The following conservation equations, written either in terms of  $P_e$  or  $h$ , demonstrate the relationship between  $K$ ,  $S_s$ , and  $D$

$$(10) \quad K_x \frac{\partial^2 P_e}{\partial x^2} = S_s \frac{\partial P_e}{\partial t} \rightarrow D \frac{\partial^2 P_e}{\partial x^2} = \frac{\partial P_e}{\partial t}$$

and

$$(11) \quad K_x \frac{\partial^2 h}{\partial x^2} = S_s \frac{\partial h}{\partial t} \rightarrow D \frac{\partial^2 h}{\partial x^2} = \frac{\partial h}{\partial t}$$

The above equations can be generalized to three dimensions. It is the goal of this research to utilize the response of hydrogeologic material to cyclic pressure signals to estimate the D or K distribution in an aquifer.

Groundwater fluctuations near coastal regions have been studied and elementary equations have been developed to associate regional groundwater levels with tidal fluctuations (Hantush, 1960). The basic mathematical description of a one-dimensional transient pressure head signal with sinusoidal boundary conditions [ $\sin(2\pi ft)$ ] is

$$(12) \quad h(r,t) = h_o e^{-d} \sin(\Phi_o - \Phi_r).$$

The head at some distance and time  $h(r,t)$  is the initial amplitude  $h_o$ , some decay term  $e^{-d}$ , multiplied by the sine of the source reference phase ( $\Phi_o=2\pi ft$ ) minus the phase shift,  $\Phi_r$ .

The amplitude decay and the phase shift depend on the ability of the aquifer to transmit the sinusoidal signal. Namely, it is the hydraulic diffusivity (D or K/Ss) of the aquifer which influences the hydraulic head measured at some distance and time from the source of a pressure head fluctuation. Three equations for the head response, within a homogeneous isotropic formation, to the migration sinusoidal boundary conditions, of excess pore pressure, have been adapted from equation (12). Equation (12) has been extended to various coordinate systems, which are presented below.

#### Linear Cartesian System

$$(13) \quad h(x,t) = h_o e^{-\sqrt{\frac{\pi f S_s}{K}} x} \sin\left(2\pi ft - \sqrt{\frac{\pi f S_s}{K}} x\right)$$

#### Cylindrical Radial System

$$(14) \quad h(r,t) = h_o \frac{e^{-\sqrt{\frac{\pi f S_s}{K}} r}}{\sqrt{r}} \sin\left(2\pi ft - \sqrt{\frac{\pi f S_s}{K}} r\right)$$

### Spherical Radial System

$$(15) \quad h(r,t) = h_o \frac{e^{-\sqrt{\frac{\pi f S_s}{K}} r}}{r} \sin \left( 2\pi f t - \sqrt{\frac{\pi f S_s}{K}} r \right)$$

Where  $t$  is time,  $x$  or  $r$  is the distance from the source,  $f$  is the frequency,  $h_o$  is the initial amplitude of the pressure head fluctuation at the source,  $S_s$  is the specific storage, and  $K$  is the hydraulic conductivity. Specific storage is the volume of fluid added or released per unit volume of aquifer per unit thickness, from compression or relaxation of the aquifer skeleton and pore due to from changes in stress. The equations (13, 14, and 15) can be thought of as two parts: the amplitude [AMP] on the right hand side

$$(16) \quad AMP = h_o \frac{e^{-\sqrt{\frac{\pi f S_s}{K}} r}}{r^*}$$

where  $r^*$  is the appropriate denominator in equations (13, 14, and 15), and the sinusoidal source phase  $\Phi_o$ ,

$$(17) \quad \Phi_o = \sin(2\pi f t) .$$

The difference in phase  $\Phi_r$  between two locations is expressed by the term

$$(18) \quad \Phi_r = -\sqrt{\frac{\pi f S_s}{K}} r = d$$

which is equal to the exponential decay term ( $d$ ) in equations (12, 13, 14, and 15). Both the amplitude decay and the degree of phase shift depend on the ratio of hydraulic conductivity to specific storage, which is the hydraulic diffusivity ( $D$ ). Estimates of  $K$  may be inferred from equation (18) to compare with other methods if  $S_s$  is assumed.



The preceding equations can be used to predict phase and amplitude versus distance for homogeneous systems, where  $K$  and  $S_s$  are constant. However, for heterogeneous systems where no analytical solutions are available, one must resort to numerical solutions. We postulate that perhaps these relatively simple formulas presented above can be used to analyze the data for heterogeneous cases by using a distance weighted average for the  $K$  (hydraulic conductivity) in the above equations. The premise is that the following replacement in the above equations might work.

$$(19) \quad \sqrt{\frac{\pi f S_s}{K}} r \Rightarrow \sum_{i=1}^I \sqrt{\frac{\pi f S_s}{K_i}} (r_i - r_{i-1})$$

The index ( $I$ ) indicates the present location of  $r$ ; so, the summation continues up to the present location of  $r$  and terminates at that point.

As indicated above, one must resort to numerical methods to calculate the phase and amplitude relations with respect to distance for heterogeneous cases where  $K$  and  $S_s$  are changing with distance. We have developed numerical models for calculating the amplitude and phase in the presence of heterogeneity for Cartesian and cylindrical coordinate systems. It was shown in the previous year's annual report (Engard et al., 2005) that this simple replacement proposed above can be used to simplify the inversion for  $K$  in certain cases. We continue to investigate the range of validity of this approximation.

As shown above, the homogeneous equations can be used to predict  $K$  based on the measurable amplitude decay and phase shift. However, the values obtained for the horizontal rays must be interpreted as spatially weighted averages over the horizontal distance between wells. Equations (14) and (15) represent the two experimental

approaches utilized in this research. The cylindrical radial equation (14) describes the behavior of the excitation of a relatively long and small radius section of screen and is considered to behave like a line source. Fully penetrating wells are often constructed at GEMS. Any test where the total screen length is excited is termed a whole well test. The spherical radial equation (15) is a representation of the point source geometry, where the excited length of well screen is relatively short. To achieve this, either a partially penetrating well with a relatively short screen length or a straddle packer apparatus must be used. A straddle packer is a double inflatable packer arrangement, which isolates a centralized interval. It would be advantageous if the packer apparatus can be deployed down typical 2 inch (5.08 cm) observation wells; so, considerable effort has been expended to design such packers.

Previous studies have shown that a line source allows for higher energy input, higher amplitudes, and increased signal propagation (Black and Kipp, 1981). A line source can create multiple ray paths to the receiver, decreasing the resolution and only approximating gross K distributions. High K material can also preferentially propagate excess pore pressures generated by a line source, which will induce a vertical gradient and cross-flow within the aquifer. Depending on the 3-D heterogeneity distribution, this cross-flow will alter the receiver signal, similar to a weighted average, again decreasing the resolution. Even high amplitude line source signals decay rapidly in the subsurface. Most of the decay is due to the exponential term in equations (14 and 15). In addition, the radial distance between source and receiver wells will cause further decay (the cylindrical or line source will additionally decay by the inverse square root of  $r$  [equation (14)] and the spherical or point source will decay by the inverse of  $r$  [equation (15)]).

These additional amplitude decay effects are due to wavefront spreading loss. However, the point source arrangement may increase the resolution of the K distribution profile because of fewer ray path possibilities.

The common component of the amplitude decay and the phase shift is  $\sqrt{\frac{\pi f S_s r}{K}}$ ;

therefore, it is possible to compare the phase data to the amplitude data [after correcting for spreading loss]. Using aforementioned assumptions, estimates of K can be obtained through algebraic manipulation. However, this method does not give a specific value for K, but rather an average ratio of  $S_s/K$  for the signal travel path from source well to receiver well. Simple theory presented here indicates that the phase and the corrected amplitude ratio should vary linearly with  $\sqrt{\frac{S_s}{K}}$  and distance (r) from the source well.

Therefore, average parameters between well pairs may be estimated. Further, if multiple source and receiver offsets (relative to their elevations) are used, multiple diagonal ray paths may be recorded. This type of testing is called hydraulic tomography (Yeh and Liu, 2000; Bohling et al., 2003), and can give more detailed information about hydraulic properties between well. In the first phase of this project we concentrated on horizontal rays where the source and receiver are at the same elevation (Zero Offset Profiles, ZOP). A ZOP survey is the simplest tomographical survey to conduct and process, but can only give information on average horizontal aquifer parameters. During the second year of this project we have started collecting diagonal ray path data (Multiple Offset Gathers, MOG). These data do show effects of heterogeneity in K, however, the processing of that data is only preliminary at this point.

## **Methodology**

### **Field Techniques**

The field scale distribution of aquifer heterogeneities govern the flow of fluid through alluvial aquifers such as GEMS. In addition, it is these heterogeneities that will dictate the retardation and/or dispersion of a contaminant species in solution with groundwater. Many methods have been developed for the purpose of understanding the dynamic behavior of an aquifer. Recent studies at GEMS have utilized custom-built straddle packers (McElwee and Butler, 1995), and pneumatic slug testing technique techniques [(McElwee and Zemansky, 2000), (Sellwood, 2001) and (Ross, 2004)].

The aquifer material at GEMS exhibits linear and non-linear responses to slug testing (Figure 5). The response of the aquifer material to the slug can be dampened such that water levels in a well return to static head conditions with time in a smooth non-oscillatory curve. However, the aquifer can be underdamped and the water levels will oscillate, decaying with time, until pre-test conditions are reached (Van Der Kamp, 1976). Theoretical advances, presented by McElwee and Zenner (1998) and McElwee (2001, 2002), have made analysis of nonlinear behavior practical and meaningful. The aforementioned slug tests are localized tests; any correlation between wells separated by some distance must be determined experimentally. Continuous layers of geologic material between tested well pairs should correlate with HRST data from each well in the well pair.

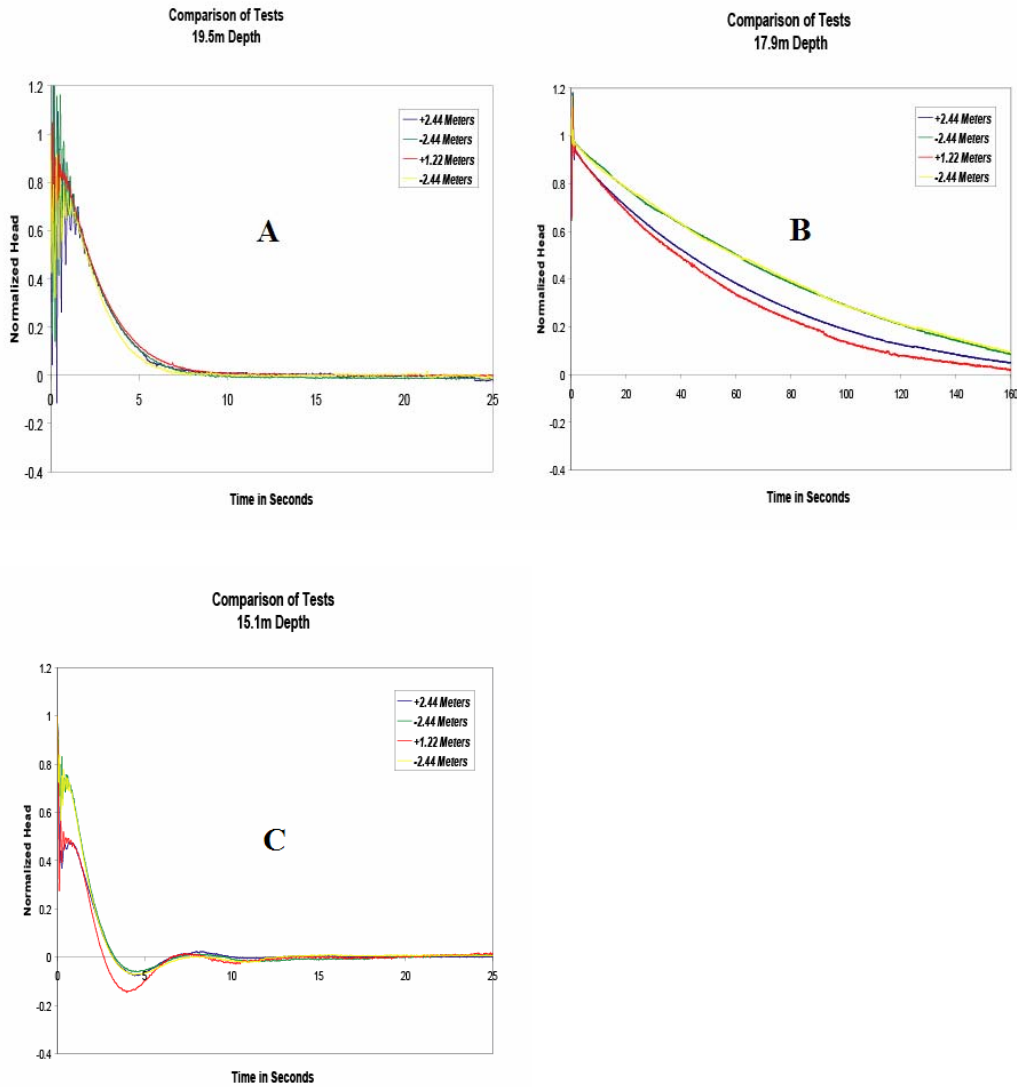


Figure 5. Three examples of slug tests performed at GEMS. Graph A displays no head dependence and behaves linearly. Graph B shows a dependence on the initial slug height and direction. Graph C is oscillatory and has some nonlinear characteristics.

The Continuous Pulse Test (CPT) is an exploratory method for extending slug test results between well pairs by propagating a sinusoidal signal. Well pairs tested and analyzed with the CPT method in this research were between 3 to 11.5 m apart. The instrumentation's ability to discern signal from noise may be a limiting factor at greater distances. As with most geophysical techniques, the equipment set up time can consume

considerable time in the field. The pneumatic CPT method takes slightly longer to perform than the typical high resolution slug test.

The continuous pulse test (CPT) was adapted from existing pneumatic slug test techniques and equipment (Figure 6). An air compressor was used to supply the driving force behind the CPT method and it was connected to an apparatus attached to the top of the casing or stand-pipe at the well. A signal generator was used to power servo-controlled valves on the apparatus, which allowed air pressure to be increased in the well or be released to the atmosphere. Increasing pressure depresses the water column, releasing the air pressure allows the water column to rebound. A single pulse of pressure is a slug test, while stacking them one after another, will create a CPT.

Typically, the aquifer at GEMS has an oscillatory response to whole well slug tests. Both linear and nonlinear recovery of water levels can oscillate about some natural frequency. The frequency and amplitude of the CPT data was adjusted to give optimal results (Engard et al., 2005, Engard, 2006).

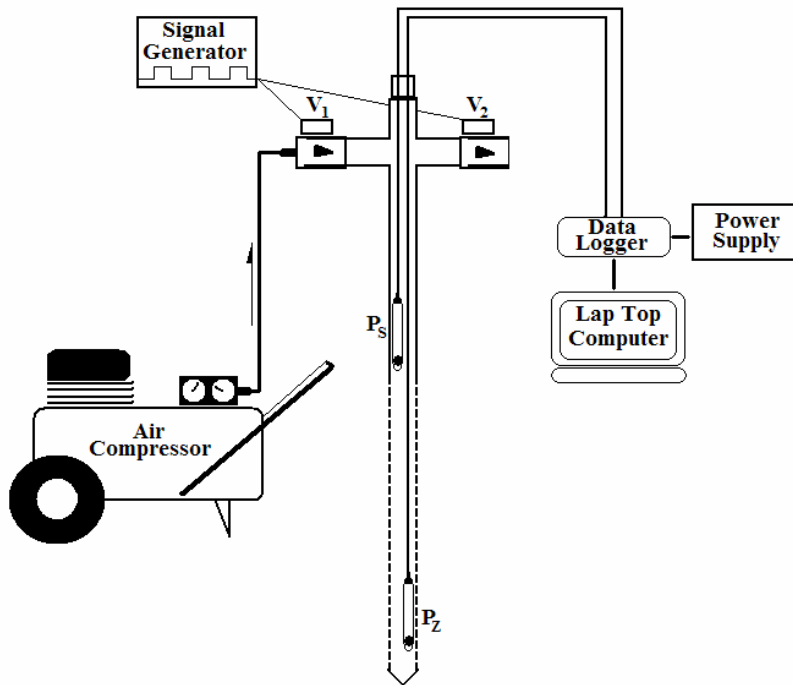


Figure 6. The pneumatic CPT equipment set up for a line source configuration. A signal generator opens and closes valves ( $V_1$  and  $V_2$ ) to control the flow of air supplied by the air compressor. The pressure transducers record the amplitude and phase at depth  $P_z$  and a reference location  $P_s$ . This setup can be easily modified for a point source configuration by using a double packer to isolate the stressed interval.

There are two geometries in which the CPT was delivered to the aquifer system, a line source and a point source. To produce a line source, the full (~9 m) extent of the source well screen was excited by increasing the head pressure in a source well. Ideally, in a homogeneous aquifer, the excess head pressure will be transferred evenly over the total length of the well screen. The point source geometry applies the excess head pressures over a relatively short section of screen. Although the stressed interval may have a much larger length than the radius, it is assumed that excess pressures will propagate approximately by spherical spreading. The double packer arrangements were custom built so they would have maximum flow-through capabilities; and once inflated,

they would block two 0.75 m sections of screen, isolating a 0.5 m interval open to the aquifer. The double packer arrangement could then be raised and lowered to stress different elevations within a fully penetrating well. As employed in a source well, fluid was injected or pneumatically driven into the aquifer through the isolated or stressed interval. Likewise, a receiver straddle packer could be raised or lowered in the observation well to monitor transient pressures at various elevations in a fully penetrating observation well.

Pressure transducers were used to monitor pressure head fluctuations in both the source well and at the observation wells. The data were collected from the pressure transducers by a data-logger and stored on a field computer for later analysis. Data were typically recorded at a 20 Hz sampling rate, which provided sufficient temporal resolution. The field computer and data logger allowed real-time monitoring of the CPT records. However, during preliminary data collection, off-site high power electrical equipment nearby produced a noisy electrical environment for recording data with the data logger. The problem was minimized by using a common grounding rod for all the data acquisition equipment.

Both the stressed interval of the source well and the isolated receiver interval in the receiver well were about 0.5 m in length. The locations BTOC were referenced to the center of the stressed or received interval. Each location center was approximately 0.3 m from the next, so that one location overlapped with the adjacent locations. The overlapping intervals acted much like a centered moving average, where the vertical changes in aquifer heterogeneity were averaged over the 0.5 m interval, but were assigned to the center point.



A custom apparatus containing six packers and five pressure ports was built to potentially speed the data collection. The pressure ports were located approximately 1 m apart isolated on either side by packers measuring approximately 0.6 m in length. The main advantage of this apparatus will come when true tomographic surveys are collected, in which multiple variable offset source and receiver locations will be measured. However, in the first year of this project the first choice of pressure transducer that was available commercially and sufficiently small was not robust enough, resulting in multiple transducer failures. In the second year of this project we tried a different set of transducers with somewhat better results. We have collected some data from this apparatus but continue to have some transducer failures. We continue to search for appropriate transducers for this multilevel sensor.

An alternate injection system to generate an oscillatory flow signal is still under development. It involves pulsed injection pumping at a packed off interval of the aquifer from a surface reservoir tank. We continue to work with this system to produce a cleaner source signal and to measure it more accurately.

## **Data Processing**

Pressure transducers are used to measure the source and receiver responses. This data was recorded via a data-logger and viewed in real time on a laptop computer during field experimentation. The data logger stored the data on the field computer hard disk as a data file.

The next step was to compute the ratio of receiver and source amplitude and the phase difference. The source and receiver amplitude and phase data are determined individually for comparison. Theory states that the decay term exponential  $d$  in equation

(12) is equal to the phase shift  $\Phi_r$ , equation (18). The phase difference, or phase shift  $\Phi_r$ , was easily computed by subtracting the source phase from the receiver phase of the fitted sine function. On the other hand, the amplitude data are a little more tedious to work with. The received amplitude divided by the source amplitude gives a ratio of amplitudes. The decay term exponential,  $d$  in equation (12), is obtained by algebraic manipulation and correction for loss. The amplitude decays as the leading edge of the source signal grows in surface area. Therefore the received amplitude data need to be corrected for the radial distance from the source. The mathematical steps to correct for spreading losses are outlined below using previously presented equations for  $h(r,t)$ .

### Cylindrical Radial System (2D)

$$(20) \quad h(r,t) = h_o \frac{e^{-\sqrt{\frac{\pi f S_s}{K}} r}}{\sqrt{r}} \sin \left( 2\pi f t - \sqrt{\frac{\pi f S_s}{K}} r \right)$$

$$(21) \quad AMP_r = h_o \frac{e^{-\sqrt{\frac{\pi f S_s}{K}} r}}{\sqrt{r}}$$

$$(22) \quad \ln \left[ \frac{AMP_r}{h_o} \sqrt{r} \right] = -\sqrt{\frac{\pi f S_s}{K}} r$$

### Spherical Radial System (3D)

$$(23) \quad h(r,t) = h_o \frac{e^{-\sqrt{\frac{\pi f S_s}{K}} r}}{r} \sin \left( 2\pi f t - \sqrt{\frac{\pi f S_s}{K}} r \right)$$

$$(24) \quad AMP_r = h_o \frac{e^{-\sqrt{\frac{\pi f S_s}{K}} r}}{r}$$

$$(25) \quad \ln \left[ \frac{AMP_r}{h_o} r \right] = -\sqrt{\frac{\pi f S_s}{K}} r$$

The details of data processing are given in Engard et al (2005) and Engard (2006). One is able to approximate the diffusivity from the final corrected amplitude derived exponential decay term  $d$  and the phase shift  $\Phi_r$ . The frequency was calculated from the field data from the reciprocal of the fitted source well period for each CPT. After referring to the literature an initial value of 0.00001 was used for  $S_s$  (Fetter, 2001; Domenico and Schwartz, 1998). Using a constant value for  $S_s$  is unrealistic but is necessary, because even with today's technology, it is difficult to measure  $S_s$  *in situ*. A final estimate of  $S_s$  was made by requiring consistency between the vertical  $K$  profiles obtained by HRST methods and CPT methods. The radial distance  $r$  can easily be measured in the field or from survey data. With some algebraic manipulation estimates of  $K$  can be made from the CPT experimentally measured phase and amplitude data. Based on the numerical results presented earlier, the CPT derived values of  $K$  should be interpreted as distance weighted averages of  $K$  over the path between the source and receiver wells. HRST  $K$  values that differ significantly from the CPT  $K$  values are evidence of inter-well heterogeneity.

## **Results From High Resolution Slug Testing and Continuous Pulse Testing**

Slug testing of an aquifer is an important tool for determining aquifer heterogeneity near a well. This type of test will average the hydraulic properties over a limited volume of aquifer. The volume of aquifer tested depends on the length of screen

in the aquifer at the tested well. A vertical profile of hydraulic conductivity distributions can be determined using high-resolution slug testing in wells (Zemansky and McElwee, 2005), or even with small diameter direct push equipment (Sellwood, 2001; Butler et al., 2002a,b; McCall et al., 2000). High-resolution slug testing enables hydrogeologists to examine vertical variations in K at a much finer scale relative to whole well slug testing.

The preferred method for initiating a multi-level slug test is to use pneumatics (Zurbuchen et al., 2002). The advantages of using pneumatics are that nothing is added to or produced from the aquifer and less equipment is needed, which is best for contaminated sites. The program NLSLUG (McElwee, 2001) based on the model presented by McElwee and Zenner (1998), was used to aid in the interpretation of oscillatory and non-oscillatory hydraulic head responses from slug testing.

For this project, high-resolution slug test (HRST) techniques were applied to newly installed wells HT-1, HT-2, and HT-3 after they were properly developed. HRST data from other wells (Ross, 2004) also was used for comparison to continuous pulse tests CPTs. A dual packer arrangement with a 0.5 m interval open to the formation was used for the slug testing.

The research presented here uses continuous, controlled, sinusoidal pressure signals as a means to estimate vertical profiles of well-to-well hydraulic diffusivity. The received signal is measured at various depths in observation wells at various distances and locations. The length of the vertical profiles measured by the CPT methods are limited by the amount of open screen common to the well pair in question and by the length of the bottom packer on the source and receiver double packer apparatus. Typically, the CPT profile was about 8 m in length.

Simple theory (the homogeneous case) predicts that the phase and log amplitude [after correcting for spherical spreading] of the sinusoidal signal should vary with  $D$  [ratio of  $K$  to specific storage ( $S_s$ )] and the radial distance,  $r$ , from the source well. The amplitude ratio [received amplitude  $AMP_r$  divided by the initial amplitude  $AMP_0$ ] and the phase difference [reference phase  $\phi_z$  minus the received phase  $\phi_r$ ] have both been measured experimentally and used to estimate the spatially averaged  $D$  between wells. Using the processing procedures outlined earlier (Engard et al., 2005; Engard, 2006), it is possible to calculate a vertical CPT  $K$  distribution.

In total, 7 line source well pairs were tested with the pneumatic CPT method at GEMS. The shortest well separation distance, 4.36 m, was between well HT-2 and well HT-3. The longest separation distance, 11.5 m, recorded was between well 00-3 and well 7-1. These results are presented in figures 7- 13. The averages of the HRST values at each depth for the source and receiver wells are plotted along with the highest and lowest values shown by error bars. This curve is labeled HRST. The other curve labeled CPT presents the results of analyzing the CPT data for  $K$ . The two curves generally agree fairly well, with the exception of figure 8. It appears that the general features of the HRST curve are captured by the CPT curve, but it seems smoother. This is probably because of the long line source geometry giving poorer resolution. It is unknown at this time why the CPT curve in figure 8 is so flat; perhaps it is due to some experimental or processing problem we have not discovered.

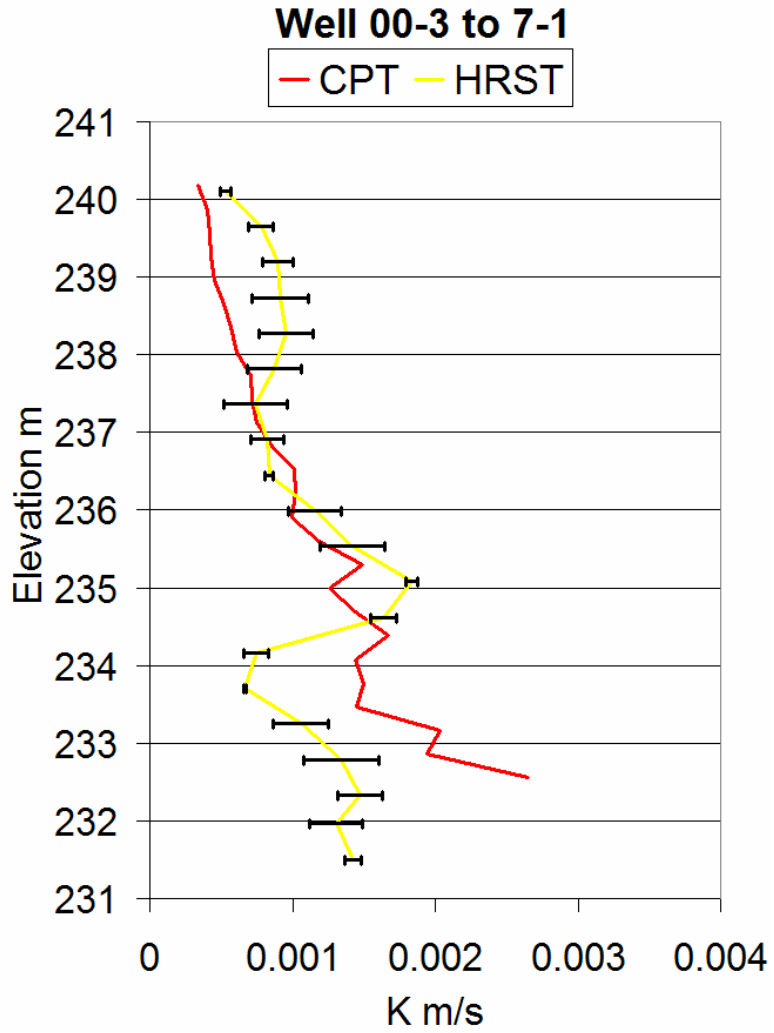


Figure 7. Comparisons of the composite HRST values from each well and the average estimated K profile from a line source pneumatic CPT between wells 00-3 to 7-1.

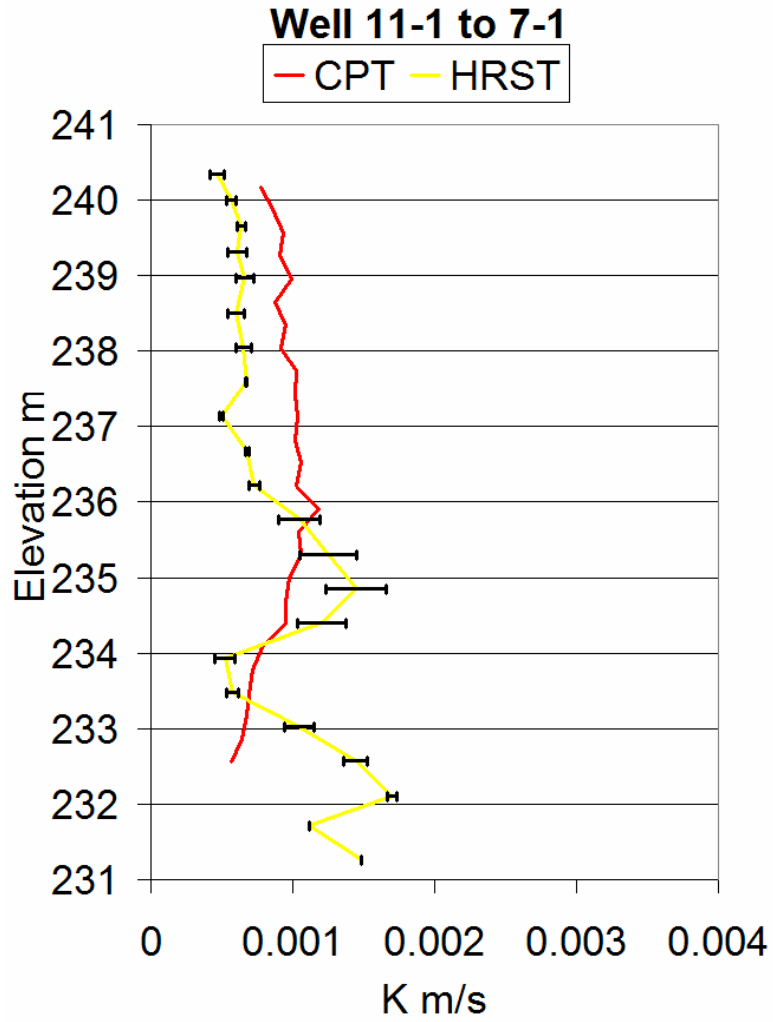


Figure 8. Comparisons of the composite HRST values from each well and the average estimated K profile from a line source pneumatic CPT between wells 00-3 to 7-1.

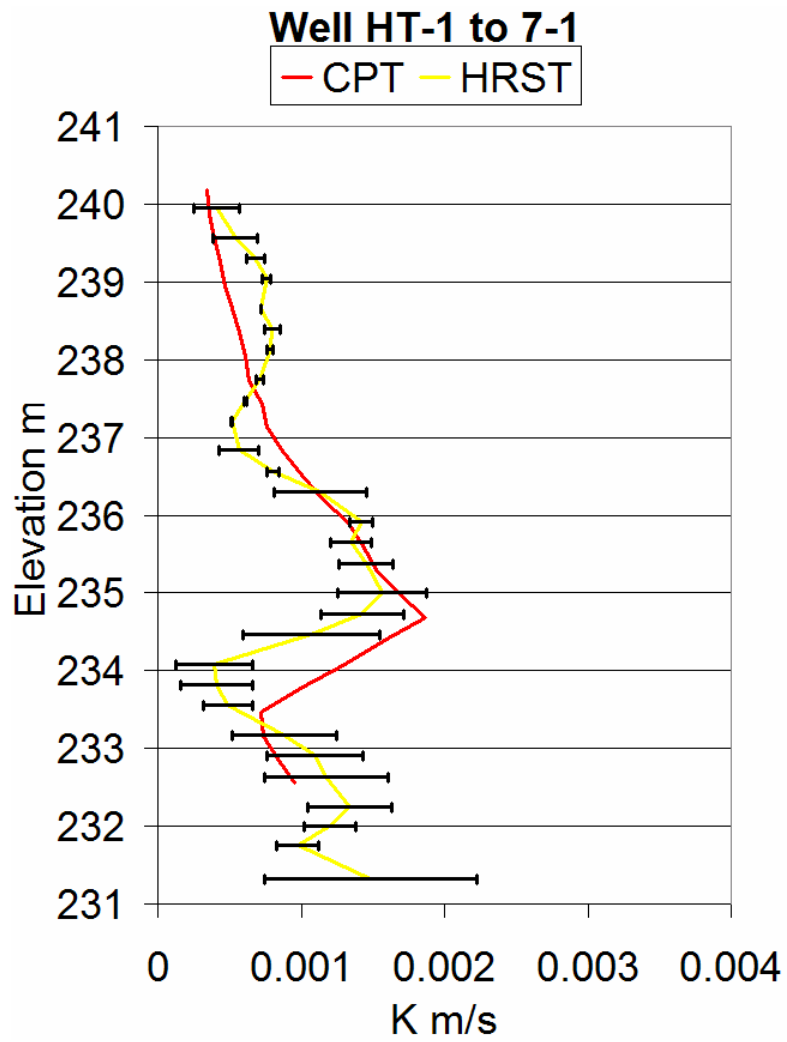


Figure 9. Comparisons of the composite HRST values from each well and the average estimated K profile from a line source pneumatic CPT between wells HT-1 to 7-1.



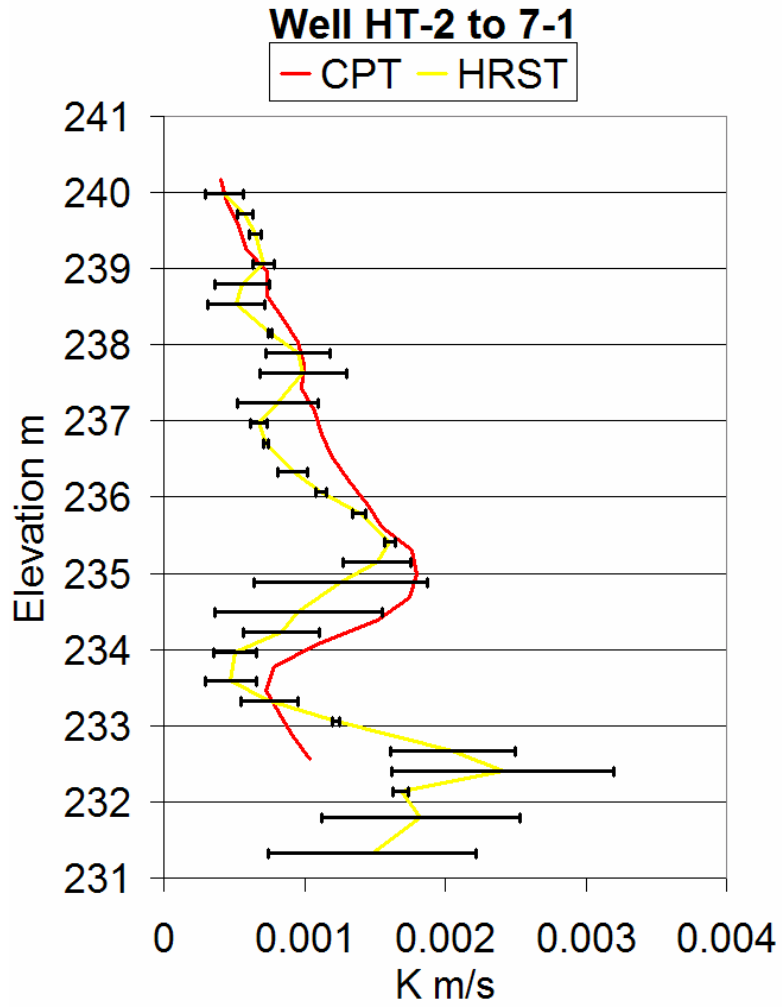


Figure 10. Comparisons of the composite HRST values from each well and the average estimated K profile from a line source pneumatic CPT between wells HT-2 to 7-1.

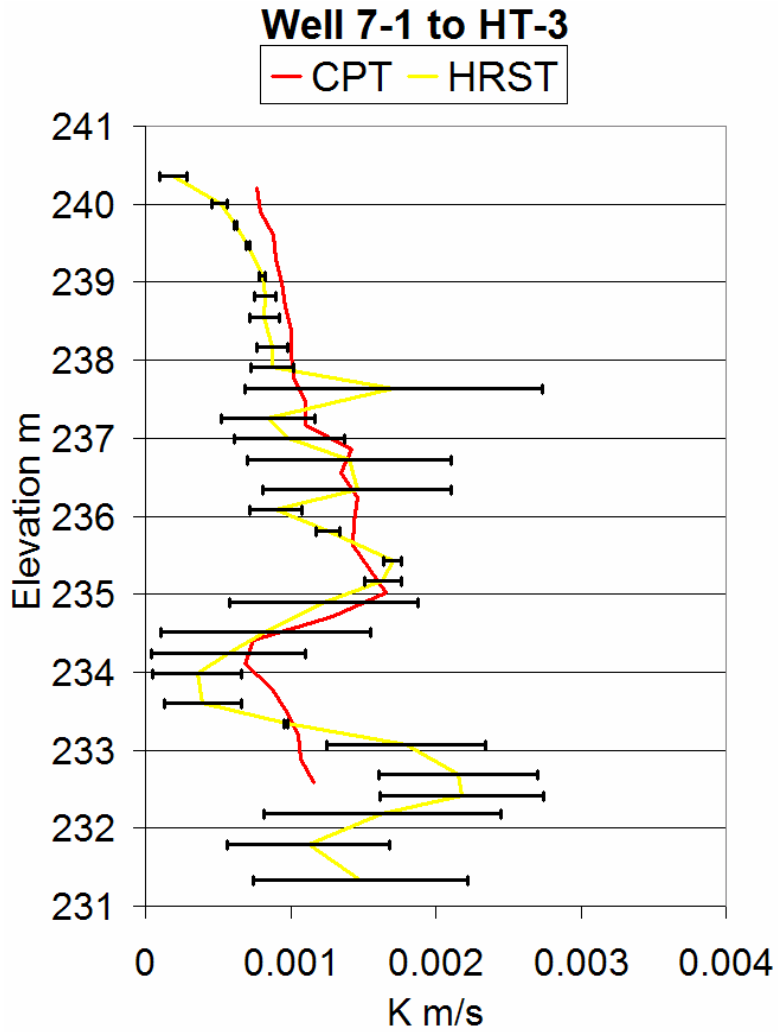


Figure 11. Comparisons of the composite HRST values from each well and the average estimated K profile from a line source pneumatic CPT between wells 7-1 to HT-3.

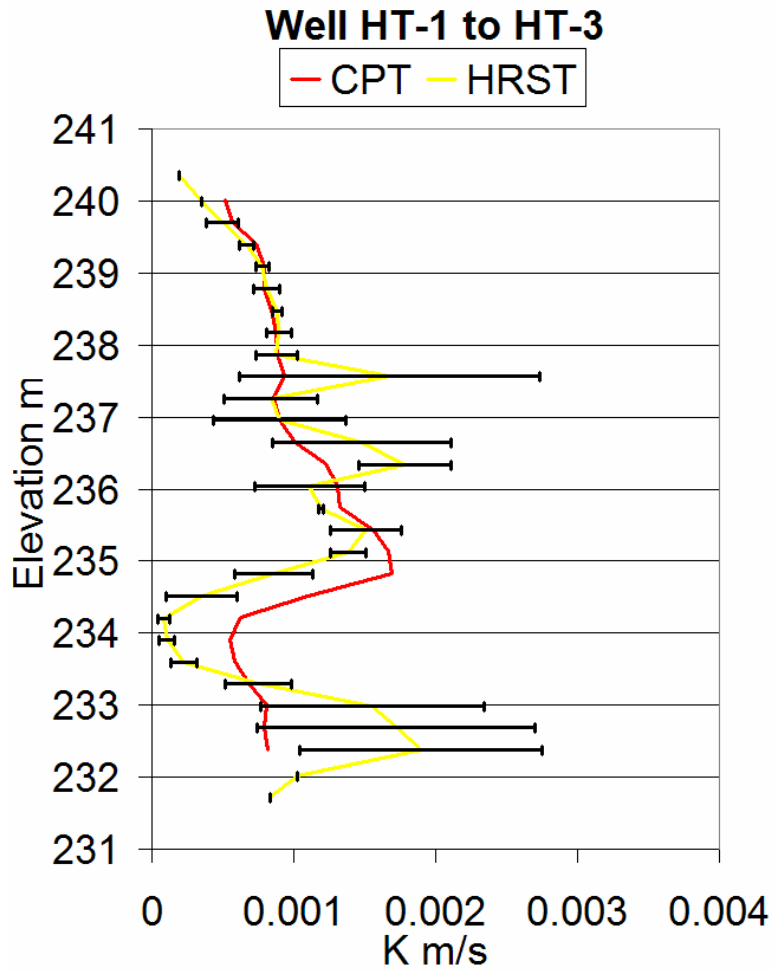


Figure 12. Comparisons of the composite HRST values from each well and the average estimated K profile from a line source pneumatic CPT between wells HT-1 to HT-3.

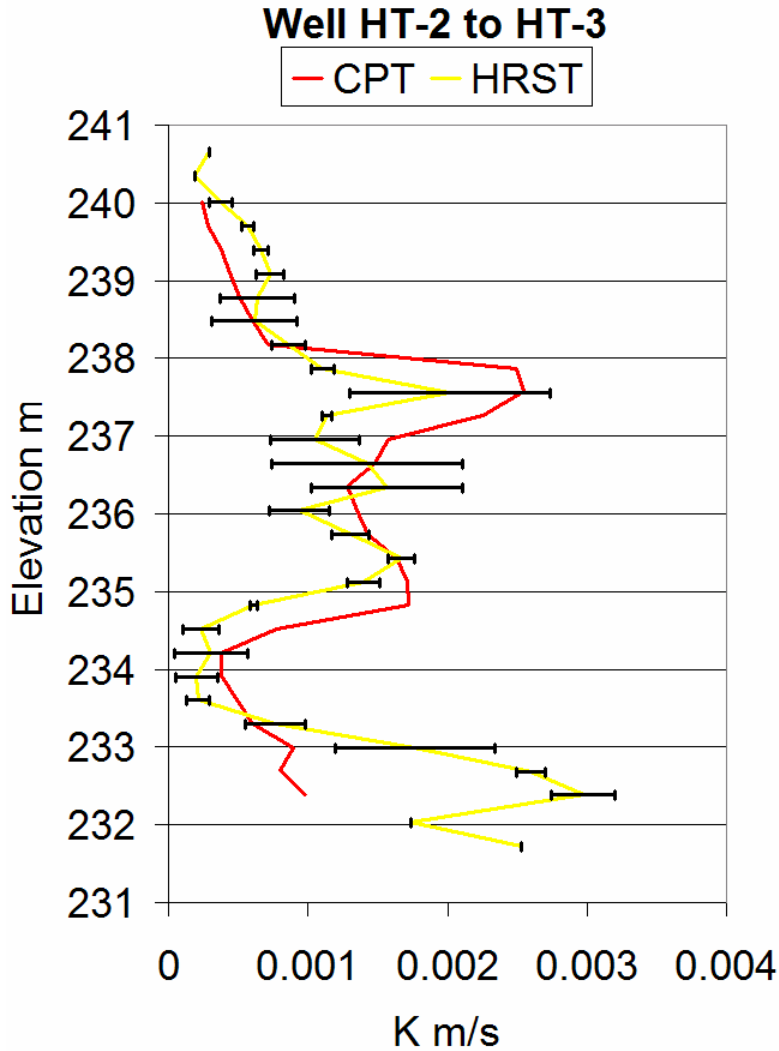


Figure 13. Comparisons of the composite HRST values from each well and the average estimated K profile from a line source pneumatic CPT between wells HT-2 to HT-3.

Five point source profiles were completed at GEMS with the pneumatic CPT method. Also, one point source profile was completed with the injection CPT method. The shortest well separation distance of 4.36 m was between well HT-2 and well HT-3. The longest separation distance, 6.91 m, was recorded between well HT-2 and well 7-1. These results are presented in figures 14- 18 for the pneumatic profiles and in figure 19

for the injection profile. The presentation style is the same as for figures 7-13 with the HRST curves being the same as before. The CPT curves are now for the point source CPT method and seem to have more detail and are more closely correlated to the HRST data. It appears that the point source CPT tests are giving better K resolution, as we might expect. Comparison of the pneumatic method of figure 14 and the injection method of figure 19 for the same well pair shows that the results are similar, but some differences do occur.

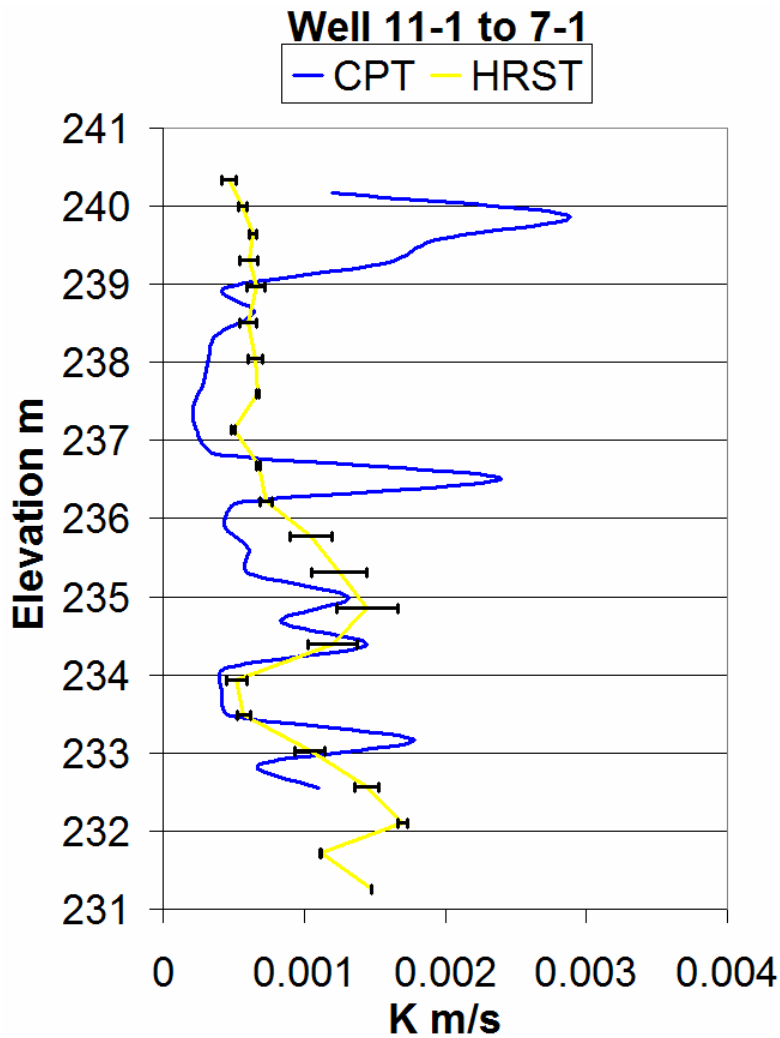


Figure 14. Comparisons of the composite HRST values from each well and the average estimated K profile from a point source pneumatic CPT between wells 11-1 to 7-1.

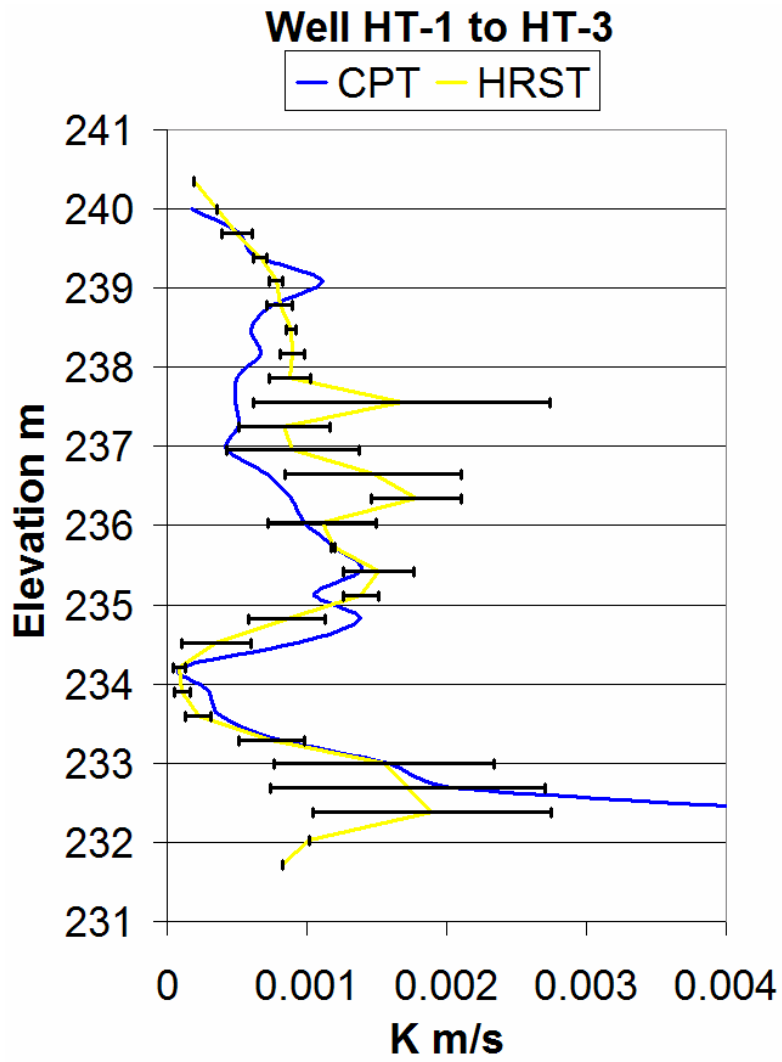


Figure 15. Comparisons of the composite HRST values from each well and the average estimated K profile from a point source pneumatic CPT between wells HT-1 to HT-3.

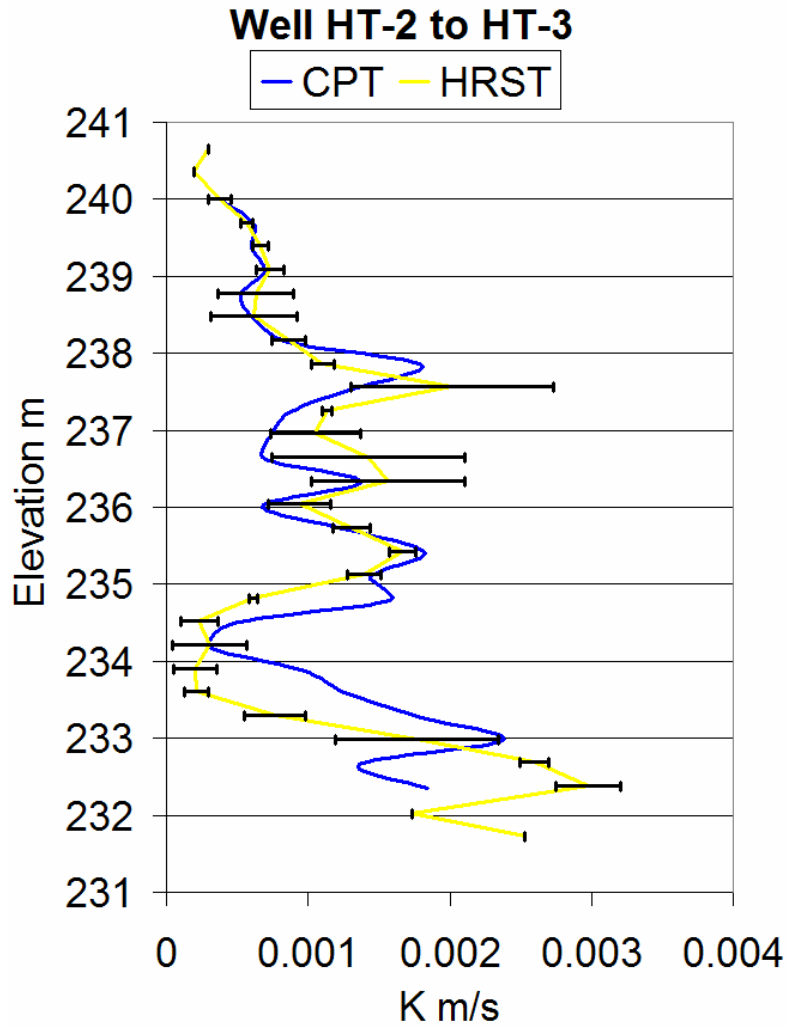


Figure 16. Comparisons of the composite HRST values from each well and the average estimated K profile from a point source pneumatic CPT between wells HT-2 to HT-3.

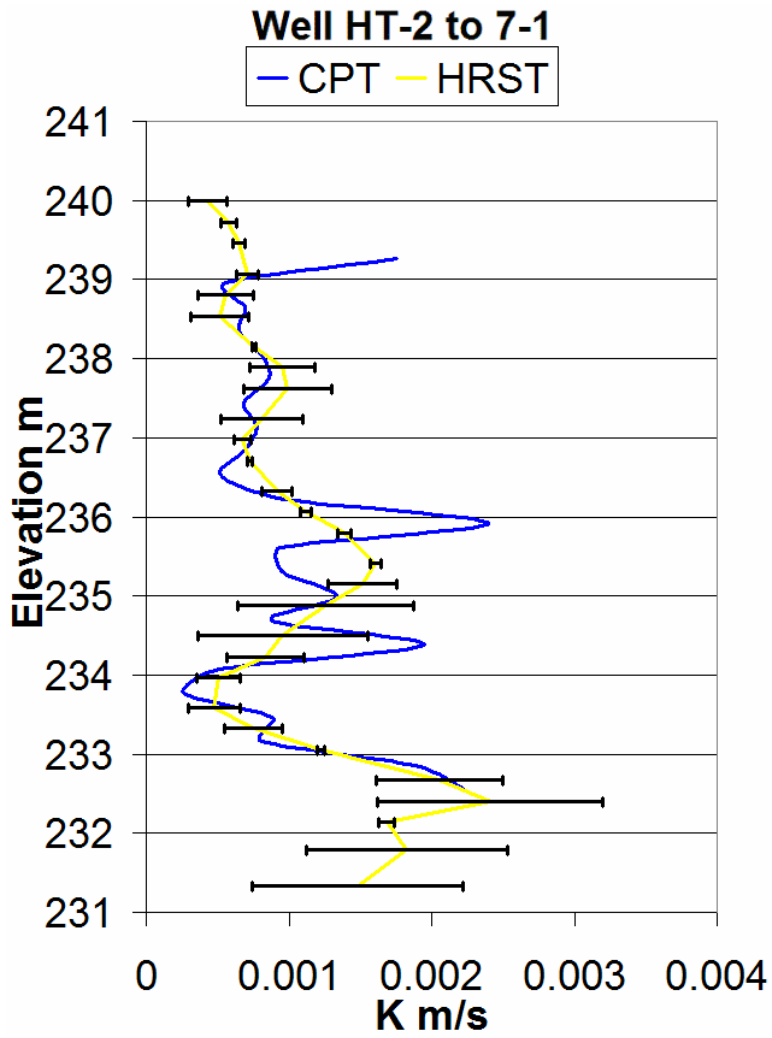


Figure 17. Comparisons of the composite HRST values from each well and the average estimated K profile from a point source pneumatic CPT between wells HT-2 to 7-1.



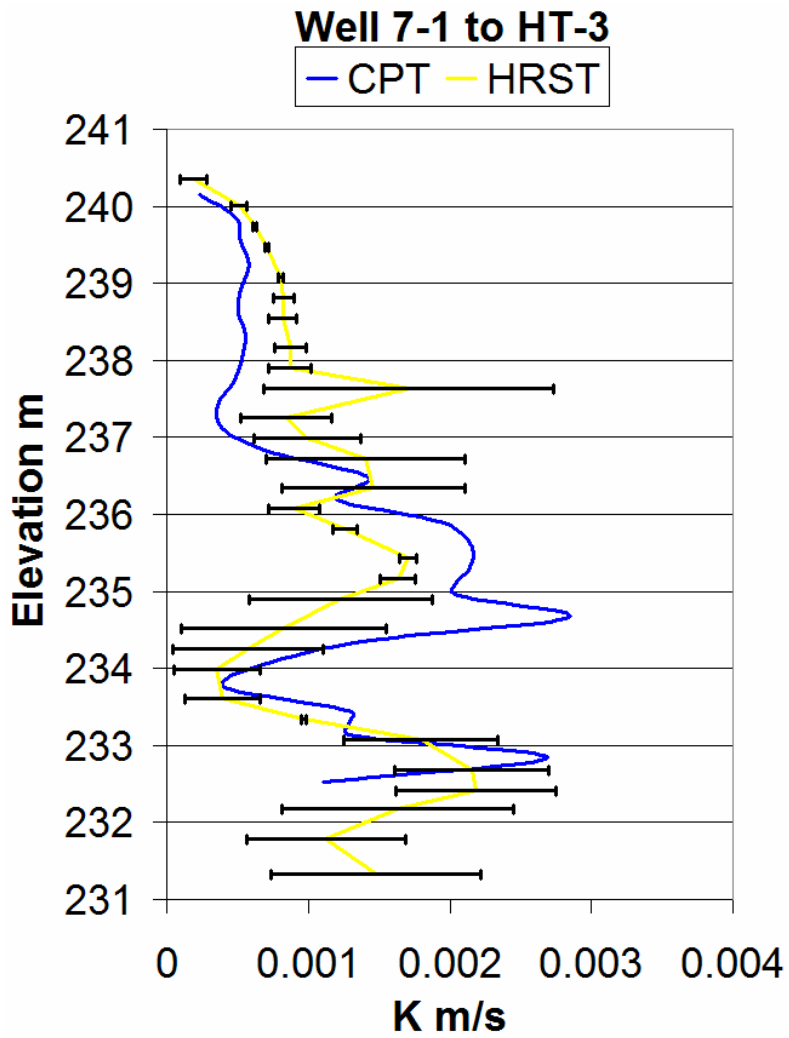


Figure 18. Comparisons of the composite HRST values from each well and the average estimated K profile from a point source pneumatic CPT between wells 7-1 to HT-3.

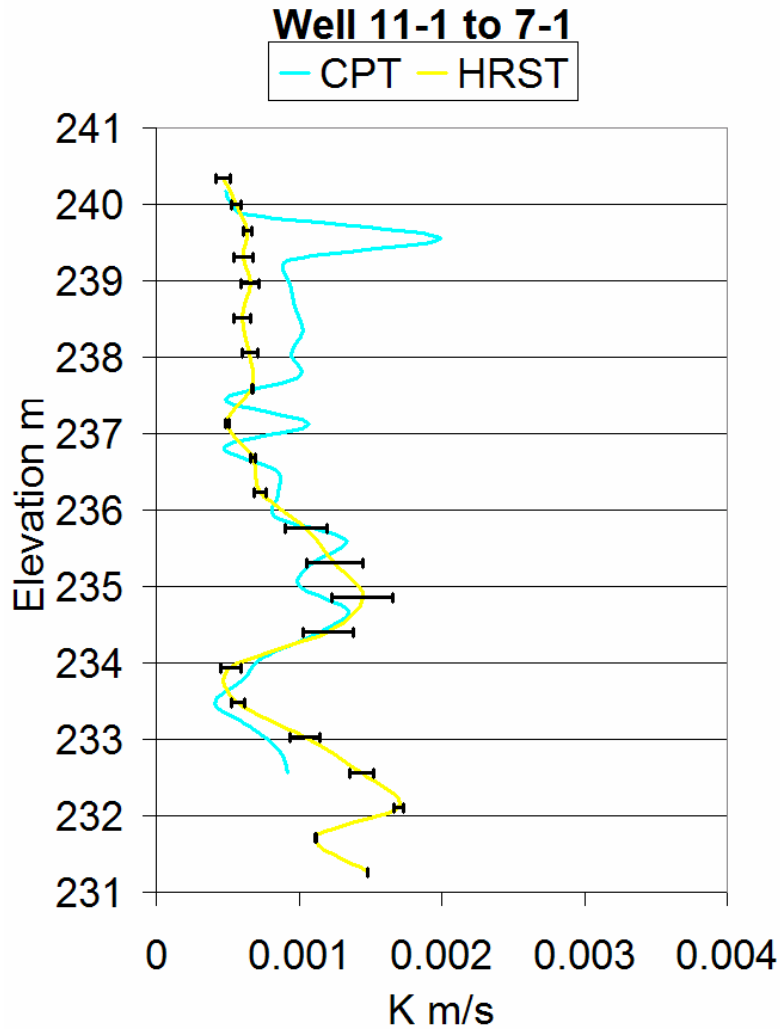


Figure 19. Comparisons of the composite HRST values from each well and the average estimated K profile from a point source injection CPT between wells 11-1 to 7-13.

It is evident that the CPT profiles mimic the general trends in the HRST K profiles measured at the respective wells. Overall, the CPT data appear to average the K profiles of the well pair in question. However, there are important differences. The heterogeneities of the geologic material between the well pair are probably the cause of this difference; and the difference can not be fully explained without using more advanced models and numerical solutions. The point source data appear to increase the

resolution of the data, distinguishing variations in K that are not present in the HRST and line source data.

### Calculation of “Anomalous K Values”

We have indicated previously that if an oscillating signal is applied to an approximately point location (packed off area) corresponding to a small part of the total thickness of the aquifer, then the response is given in the radial spherical system by equation (15) or (23):

$$h(r,t) = h_o \frac{e^{-\sqrt{\frac{\pi f S_s}{K}} r}}{r} \sin \left( 2\pi f t - \sqrt{\frac{\pi f S_s}{K}} r \right)$$

Notice that the amplitude decays as the inverse of the radial distance from the point source to the receiver.

The above equation can be used to predict phase and amplitude of the received signal versus distance for homogeneous systems, where K and S<sub>s</sub> are constant. However, for heterogeneous systems where no analytical solutions are available, one must resort to numerical solutions.

We postulated earlier that perhaps this relatively simple formula presented above can be used to analyze the data for heterogeneous cases by using a distance weighted average for the K (hydraulic conductivity) in the above equation. The premise is that the following replacement in the above equation might work [equation (19)].

$$\sqrt{\frac{\pi f S_s}{K}} r \Rightarrow \sum_{i=1}^I \sqrt{\frac{\pi f S_s}{K_i}} (r_i - r_{i-1})$$

The index “I” indicates the present location of  $r$ ; so, the summation continues up to the present location of  $r$  and terminates at that point. Since we do not have analytical solutions for the heterogeneous case, we must resort to numerical methods to see if the above replacement works. We have developed numerical models for calculating the amplitude and phase in the presence of heterogeneity for Cartesian and cylindrical coordinate systems. We have not completed the development for the spherical system yet.

As was shown in the previous year annual report (Engard et al., 2005), the agreement between the numerical data for heterogeneous systems and the theory using a spatially weighted average to solve for  $K$  is excellent, except near boundaries and near the origin. The calculated values for  $K$  were determined by considering the phases from the numerical models. The results for  $K$  using the amplitude data are similar but have a little more error near the origin.

The above results indicate that using a spatially weighted average for  $K$  should be appropriate. This allows the interpretation of the hydraulic conductivity ( $K$ ) data that has been collected for high-resolution slug tests at wells and the inter-well spatially averaged  $K$  that has been determined by the continuous pulse testing horizontal ray path data. Unfortunately, there is no unique way to do the spatial weighting with the horizontal ray path data, since we only have one ray path crossing each segment of the aquifer. When we are able to collect diagonal ray path data, we will have multiple rays that cross each given segment of the aquifer and it will be possible to estimate the spatial averaging to some scale limited by the density of ray paths. However, in the present case (horizontal ray path data) one must assume some spatial averaging scheme to interpret what the inter-

well average K is telling us about the variation of K between wells. It is well known that slug tests only give a K value that is representative near the well. Therefore, we should give less weight the slug test values and more weight to the inter-well average K determined from the horizontal ray-path data. Arbitrarily, let us assume that the weight for each of the two slug test values is 1/6 and the weight for the inter-well average K is  $2/3 = 4/6$ . These weighting coefficients add up to 1, as any weighting scheme should. This assumption will allow us to calculate a new value of K between the source and receiver wells that may be different from the slug test K values or the inter-well average K determined from the horizontal ray path data. In what follows we will call this calculated value of K between the source and receiver wells the “anomalous K value” because it can be different from any of the experimentally determined K values. Ideally, if the K values changed in a linear fashion from the source well to the receiver well, the inter-well average K determined from the horizontal ray path data should fall between the values of K determined by slug tests at each well. However, we have observed that this often is not the case, which means that the K values are not varying linearly between wells. The above outlined scheme allows us to calculate an “anomalous K value” that shows how K may in fact be varying between wells.

This procedure has been applied to three of the source-receiver well pairs from which we have collected data. The calculations for the Well pairs HT-1 to HT-3, HT-2 to HT-3, and 7-1 to HT-3 are show in figures 20, 21, and 22 respectively. What we observe is that the inter-well average K (CPT K value in the figures, shown in dark blue) is many times outside the interval defined by the two slug test values of K shown in pink and yellow. This means that the K value is not varying linearly between wells and an

anomalous value outside that range may be calculated. The anomalous values are shown in light blue-green. When the anomalous curve is significantly outside the slug test K interval, we have an indication that the K value between wells is significantly different from that observed at the source and receiver wells. The values of the anomalous K are calculated using the weighting scheme detailed earlier. It should be reiterated that the choice of weighting scheme is arbitrary at this point and is not unique. However, the calculations presented here should be useful in identifying areas of “anomalous K” between the source and receiver wells.

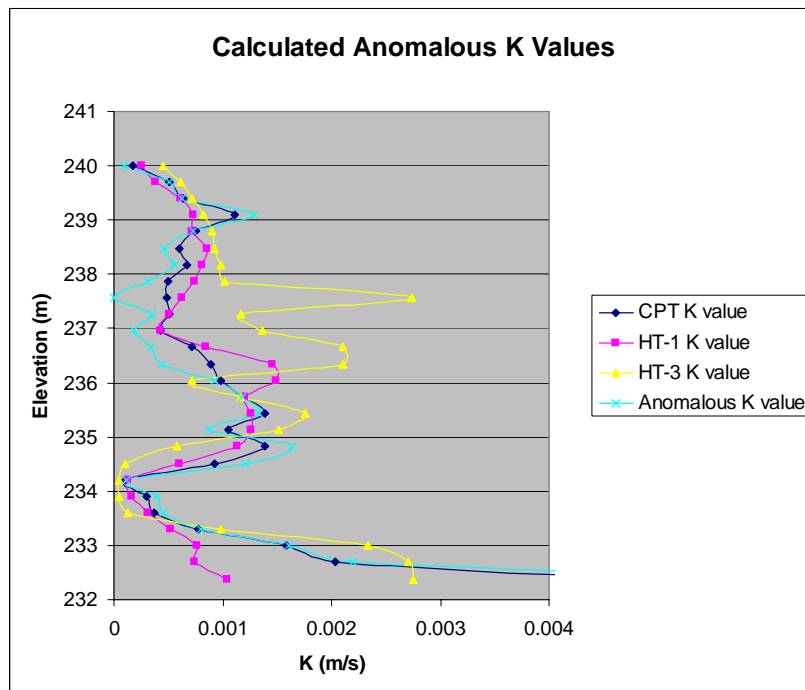


Figure 20. Experimentally determined K values from high resolution slug tests and horizontal ray path data along with “anomalous K values” calculated from the weighting scheme, for well pair HT-1 and HT-3.

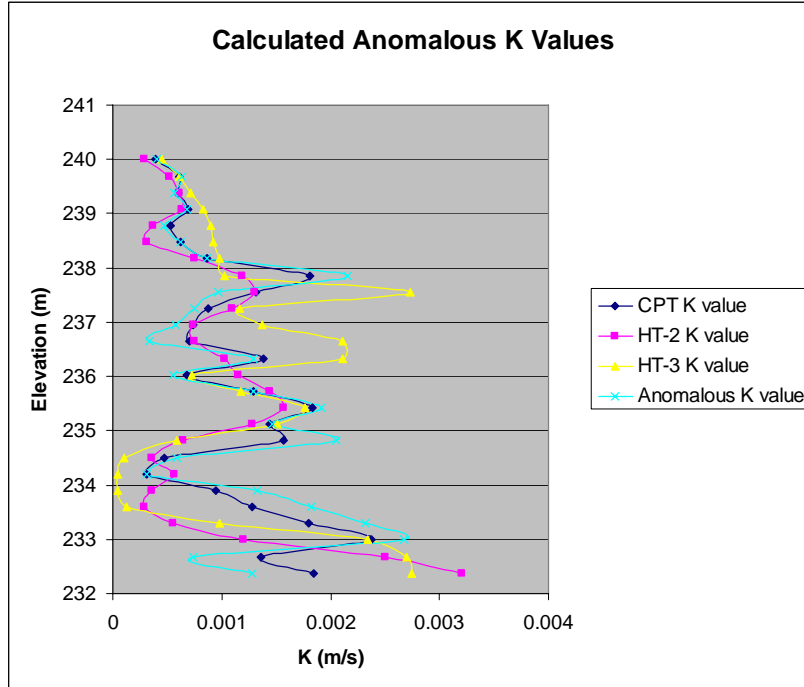


Figure 21. Experimentally determined K values from high resolution slug tests and horizontal ray path data along with “anomalous K values” calculated from the weighting scheme, for well pair HT-2 and HT-3.

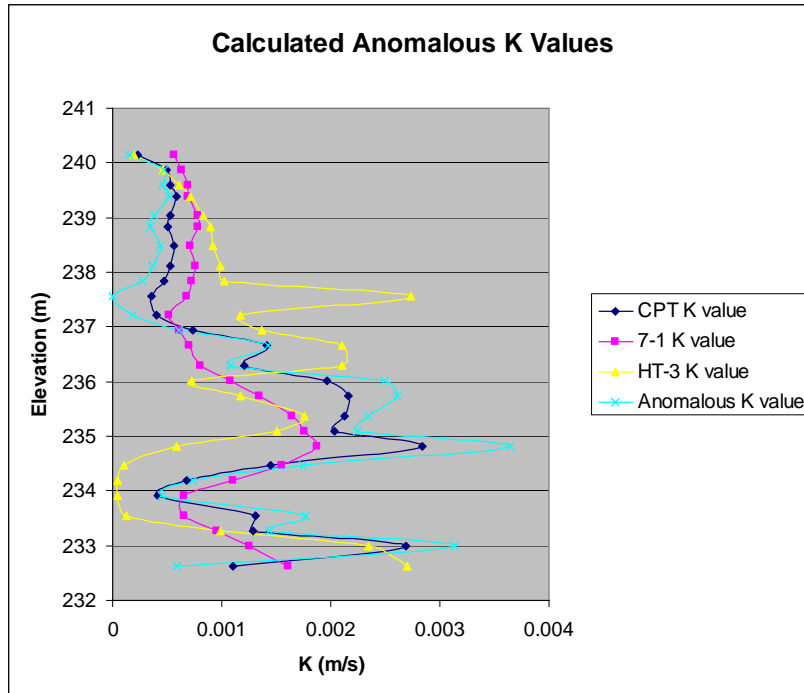


Figure 22. Experimentally determined K values from high resolution slug tests and horizontal ray path data along with “anomalous K values” calculated from the weighting scheme, for well pair 7-1 and HT-3.

## Reproducibility and Reciprocity

We have investigated the reproducibility of the data and the reciprocity of source and receiver wells. In well pair HT-1 and HT-3 we have taken data at two different times and with the source and receiver locations reversed. The results are shown in Figure 23 for the measured phase which is the basic data used to calculate K. It is seen that the signals are reproducible within experimental error over an extended time interval between data collection and with the source and receiver reversed. Similarly, for well pair HT-2 and HT-3 we have taken data at four different times and once with the source and receiver reversed. These data sets are shown in Figure 24. The general shape and features of the phase shift curve are reproduced and the various data sets agree within experimental accuracy. Therefore, we conclude that the data is reproducible and that it is nearly independent of source and receiver position, within experimental error.

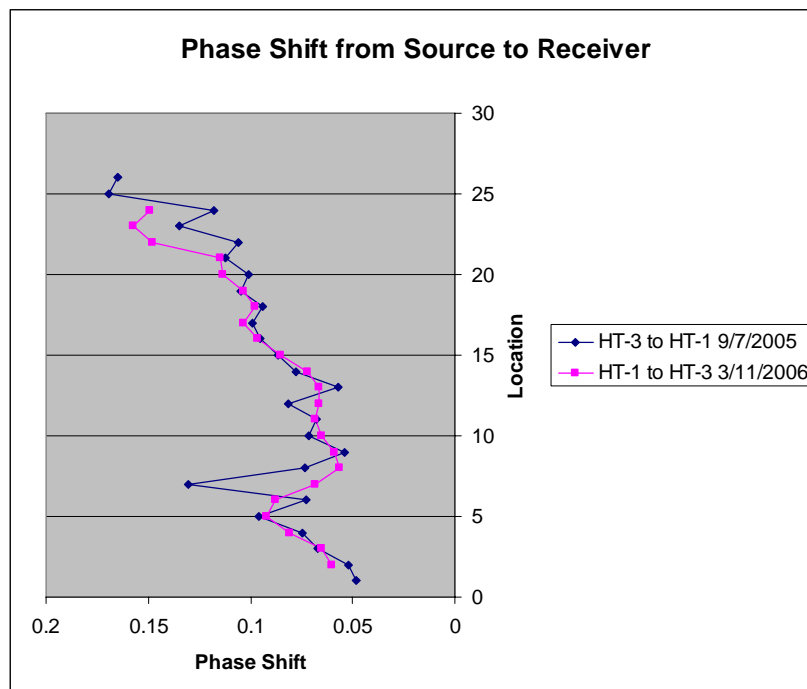


Figure 23. Phase data for well pair HT-1 and HT-3 at two different times with the source and receiver reversed.



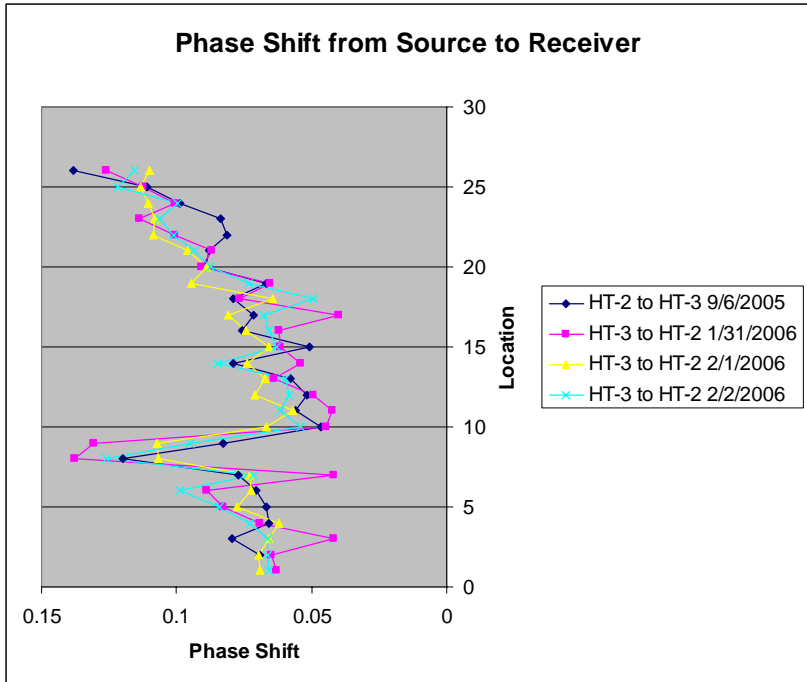


Figure 24. Phase data for well pair HT-2 and HT-3 at four different times with the source and receiver reversed on one data set.

### Diagonal Ray Path Data

In the second phase of this work we have begun to collect diagonal ray path data. In the previous work shown in this paper we have been using horizontal ray path data where the source and receiver are located at the same elevation. In that case, only an average horizontal hydraulic conductivity at that elevation may be computed. Ultimately, we want to collect multiple ray path data so that tomographic techniques can be used to estimate the lateral and vertical distribution of hydraulic conductivity between the source and receiver wells. We have collected a number of data sets where the source is fixed and the receiver location varies throughout the vertical extent of the receiver well screen (MOG, multiple offset gather). Such a data set is shown in figure 25, where the source location is shown and the vertical axis of the graph indicates the receiver locations. The

measured phase shift is shown by the blue curve and the yellow curve shows the theoretical phase shift that would occur as a function of radial distance if the aquifer was homogeneous. Clearly, the data are showing phase deviations due to heterogeneity. The smallest phase shift corresponds to the highest measured hydraulic conductivity and the largest phase shift indicates a much lower hydraulic conductivity. The graph shows that there is a zone of near homogeneous hydraulic conductivity near the source elevation. The lowest indicated hydraulic conductivity is near the top of the graph as we approach the overlying silt and clay layer. As we move below the source location the hydraulic conductivity also decreases. This zone of lower K at about 234 m is also seen in the horizontal ray path data shown in figures 14-18.

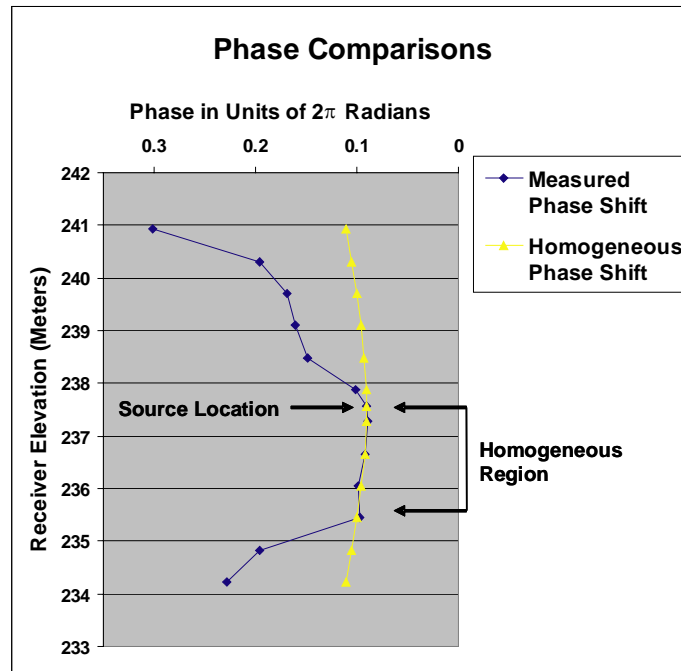


Figure 25. Experimentally measured phase shift for a MOG for a well pair and the calculated homogeneous phase shift due only to variations in radius.

## Summary and Conclusions

The primary objective of the first phase of this project was to determine the effectiveness of horizontal pulse testing to obtain better estimates of aquifer parameters. To accomplish this goal, several things had to be done. First, a theoretical and a numerical framework was needed to describe the propagation of a sinusoidal signal. Applying the theory to a real field study site required the development of new equipment and field procedures. To analyze the results of field experiments, a processing scheme was developed.

The distinct advantage of using a sinusoidally varying source is that the intrinsic response of the geologic material is measured by the amplitude and phase of the received sine wave. Two types of source geometries were used: the whole well line source and the isolated point source. The line source introduces a greater amount of energy, and therefore has a greater propagation distance than the point source. On the other hand, the point source geometry allows for a better vertical resolution of the aquifer characteristics.

The success of data processing for these experiments depended on the theoretical framework presented earlier. The prediction of groundwater fluctuations from sinusoidal tidal fluctuations was adapted to our local scale experiments. This framework made it possible to estimate the diffusivity ( $D$ ) of the aquifer material, the ratio the hydraulic conductivity ( $K$ ) to the specific storage ( $S_s$ ), from the ratio of measured amplitudes and the phase shift. An empirical correction was made to normalize the mean CPT estimated  $K$  values to the mean HRST  $K$  values. In effect, this correction changed the specific storage estimate in the ratio of  $K/S_s$  from its original estimate obtained from the literature.

The HRST methods used here are able to measure the vertical profile of changes in aquifer characteristics near a particular well. HRST data for several wells in an area may shed some light on the stratification of horizontally deposited geologic units by looking at correlations of various K layers between pairs of wells. There is no physical measurement on the aquifer material between the well pair; therefore, it is only possible to make a linear interpolation between two measured wells for HRST data. The CPT method was designed to bridge the gap between HRST measurements made at individual wells. Even without adjusting  $S_s$ , the line source and the point source CPT derived estimates of  $K$  reflect the general trend in hydrogeological conditions measured by HRST methods.

As detailed in the previous results section, 7 pneumatic line source CPT profiles and 6 point source CPT profiles were completed at GEMS. The line source method was the simplest arrangement to deploy and data could be collected faster from the well pair. To conduct a point source CPT, an additional packer apparatus had to be assembled, deployed, and moved periodically, which increased the field experiment time. Although once set up, the point CPT profile can be completed relatively quickly. The range of radial distances between tested well pairs was 1.5 to 11.5 m.

The data presented here show that the CPT profiles mimic the general trends in the HRST K profiles measured at the respective wells. Overall, the CPT data appear to average the K profiles of the well pair in question. However, there are important differences. The heterogeneities of the aquifer between the well pair are probably the cause of this difference; and the difference can not be fully explained without using more advanced models and numerical solutions. We have made an elementary attempt at

calculating “anomalous K values” between well pairs. Both the line source data and the point source data appear to distinguish variations in K that are not present in the HRST data. However, the point source data appear to have the best resolution of the data presented here. Experiments indicate that the data are reproducible at different times and with the source and receiver wells reversed, within experimental accuracy.

The CPT method shows promise as a hydrogeological tool. The interpretation of the ZOP CPT data presented here is limited to vertical changes in the mean horizontal aquifer parameters, which are assumed to be given by linear interpolation between wells. To obtain more detail on K variations between well pairs, hydraulic tomography may be applied to the CPT method. Hydraulic tomography uses multiple vertical offsets between source and receiver locations. It uses an inversion technique to estimate parameters for a 2-D vertical slice of the distribution of aquifer heterogeneities (Yeh and Liu, 2000). We have begun collecting diagonal ray path data and it shows variations attributable to aquifer heterogeneity. Future research on this project will deal with development of numerical models necessary for interpreting tomographical data and with development of appropriate experimental data collection techniques for tomography.

## References

- Barker, J.A., 1988. A generalized radial flow model for hydraulic tests in fractured rock. *Water Resources Research* 24. No. 10:1796-1804.
- Black, J.H., and Kipp, K.L. 1981. Determination of hydrogeological parameters using sinusoidal pressure tests: A theoretical appraisal. *Water Resources Research* 17. No. 3:686-692.
- Bohling, G.C., 1999. Evaluation of an induced gradient tracer test in an alluvial aquifer, Ph.D. Dissertation, University of Kansas, 224 p.
- Bohling, G.C., Zhan, X., Knoll, M.D., Butler J.J. Jr. 2003. Hydraulic tomography and the impact of a priori information: An alluvial Aquifer Example. *Kansas Geological Survey Open-file Report 2003-71*
- Brauchler, R., Liedl, R., Dietrich, P., 2001. A travel time based hydraulic tomographic approach. *Water Resources Research* 39. No. 12:1-12
- Bredehoeft, J.D and Papadopoulos, S.S. 1980. A method for determining the hydraulic properties of tight formations. *Water Resources Research* 16. No. 1:233-238
- Butler, J.J. Jr., Garnett, E.J., Healey, J.M. 2002a. Analysis of slug tests in formations of high hydraulic conductivity. *Ground Water* 41. No. 5:620-630
- Butler, J.J. Jr., J.M. Healey, G.W. McCall, E.J. Garnett, and S.P. Loheide II. 2002b. Hydraulic tests with direct-push equipment. *Ground Water* 40, No. 1:25-36
- Cooper, H.H., Bredehoeft, J.D., Papadopoulos, I.S., and Bennett, R.R. 1965. The response of well-aquifer systems to seismic waves. *Journal of Geophysical Research* 70, No. 16:3915-3926
- Domenico, P., and Schwartz, F. 1998. *Physical and chemical hydrogeology*. 2<sup>nd</sup> Ed. John Wiley & Sons. New York, New York.
- Engard, B., 2006, Estimating Aquifer Parameters From Horizontal Pulse Tests, Masters Thesis, University of Kansas, 107 pp.
- Engard, B., McElwee, C.D., Healey, J.M., and Devlin, J.F., 2005, Hydraulic tomography and high-resolution slug testing to determine hydraulic conductivity distributions: Kansas Geological Survey Open File Report #2005-36, 81 p.
- Fetter, C.W., 2001. *Applied Hydrogeology*. 4<sup>th</sup> Ed. Prentice Hall. Upper Saddle River, New Jersey.

Ferris, J.G., 1951. Cyclic fluctuations of the waterlevels as a basis for determining aquifer transmissivity, *IAHS Publ.*, 33, p. 148-155.

Hantush, M.S., 1960. Lectures at New Mexico Institute of Mining and Technology. unpublished, compiled by Steve Papadopoulos, 119 p.

Healey, J., McElwee, C., and Engard, B., 2004. Delineating hydraulic conductivity with direct-push electrical conductivity and high resolution slug testing. *Trans. Amer. Geophys. Union* 85, No.47: Fall Meet. Suppl., Abstract H23A-1118.

Huettl, T.J., 1992. An evaluation of a borehole induction single-well tracer test to characterize the distribution of hydraulic properties in an alluvial aquifer. Masters Thesis, The University of Kansas.

Jiang, X., 1991. Field and laboratory study of the scale dependence of hydraulic conductivity. Masters Thesis, The University of Kansas.

Jiao, J.J. and Tang, Z., 1999. An analytical solution of groundwater response to tidal fluctuation in a leaky confined aquifer. *Water Resources Research* 35. No. 3:747-751

Johnson, C.R., Greenkorn, R.A., and Woods, E.G., 1966. Pulse-Testing: A new method for describing reservoir flow properties between wells. *Journal of Petroleum Technology*. (Dec1966) pp. 1599-1601.

Lee, J., 1982. Well Testing. Society of Petroleum Engineers of AIME, New York. 156 p.

McCall, W., Butler J.J. Jr., Healey, J.M., and Garnett, E.J., 2000. A dual-tube direct push method for vertical profiling of hydraulic conductivity in unconsolidated formations. *Environmental & Engineering Geoscience* Vol. VIII, no. 2:75-84

McElwee, C.D., 2001. Application of a nonlinear slug test model. *Ground Water* 39. No. 5:737-744

McElwee, C.D., 2002. Improving the analysis of slug tests. *Journal of Hydrology* 269:122-133

McElwee, C.D., and Butler, J.J. Jr., 1995. Characterization of heterogeneities controlling transport and fate of pollutants in unconsolidated sand and gravel aquifers: Final report. Kansas Geological Survey open file report 95-16.

McElwee, C.D., and Zenner, M.A., 1998. A nonlinear model for analysis of slug-test data. *Water Resources Research* 34. No. 1:55-66.

Novakowski, K.S., 1989. Analysis of pulse interference tests. *Water Resources Research* 25. No. 11:2377-2387

Pierce, A., 1977. Case history: Waterflood performance predicted by pulse testing. *Journal of Petroleum Technology*. (August 1977) 914-918.

Ross, H.C. 2004. Utility of multi level slug tests to define spatial variations of hydraulic conductivity in an alluvial aquifer, northeastern Kansas. Masters Thesis, The University of Kansas.

Schad, H., and Teutsch, G., 1994. Effects of scale on pumping test results in heterogeneous porous aquifers. *Journal of Hydrology* 159. pp. 61- 77.

Schulmeister, 2000. Hydrology and geochemistry of an alluvial aquifer near a flood plain margin. Dissertation, University of Kansas.

Schulmeister, M.K., Butler, J.J. Jr., Healey, J.M., Zheng, L., Wysocki, D.A., and McCall, G.W., 2003. Direct-Push Electrical Conductivity Logging for High-Resolution Hydrostratigraphic Characterization. *Ground Water Monitoring & Remediation* 23. No. 3:52-62.

Sellwood, S., 2001. A direct-push method of hydrostratigraphic site characterization. Masters thesis, The University of Kansas.

Van Der Kamp, G., 1976. Determining aquifer transmissivity by means of whole well response tests: The underdamped case. *Water Resources Research* 12. No. 1:71-77.

Yeh, T.C., and Liu, S., 2000. Hydraulic tomography: Development of a new aquifer test method. *Water Resource Research* 36. No. 8:2095-2105

Zemansky, G.M., and McElwee, C.D., 2005. High-Resolution Slug Testing. *Ground Water* 43. No. 2: 222-230

Zurbuchen, B.R., Zlotnik, V.A., and Butler, J.J. Jr., 2002. Dynamic interpretation of slug tests in highly permeable aquifers. *Water Resources Research* 38. No. 3:1-17



## Appendix A. Technical Publications

### Published Abstracts.

Healey, J. M., McElwee, C. D., and Engard, B., 2004, Delineating hydraulic conductivity with direct push electrical conductivity and high-resolution slug testing: *Eos, Trans. Amer. Geophys. Union*, v. 85, no 47, Fall Meet. Suppl., Abstract H23A-1118, p. F773.

Engard, B. and McElwee, C. D., 2005, Continuous pulse testing for estimating aquifer parameters: *Proceedings 50<sup>th</sup> Annual Midwest Ground Water Conference*, Nov. 1-3, Urbana, Illinois.

Engard, B. and McElwee, C. D., 2005, Estimating aquifer parameters from oscillatory well stresses: *Proceedings SERDP Partners in Environmental Technology Technical Symposium and Workshop*, Nov. 29-Dec. 1, Washington, D.C., p. G-26.

Engard, B. and McElwee, C. D., 2005, Estimating hydraulic conductivity: Hydraulic tomography and high-resolution slug tests: *Eos, Trans. Amer. Geophys. Union*, 86(52), Fall Meet. Suppl., Abstract H21C-1359.

McElwee, C. D. and Engard, B., 2006, Using Oscillatory Pressure Waves to Measure Hydraulic Conductivity Distributions: *Proceedings SERDP Partners in Environmental Technology Technical Symposium and Workshop*, Nov. 28-30, Washington, D.C.

McElwee, C. D. and Engard, B., 2006, Hydraulic Tomography Using Oscillatory Pressure Waves: *Eos, Trans. Amer. Geophys. Union*, 87(52), Fall Meet. Suppl., Abstract H41B-0382.

### Annual Report

Engard, B., McElwee, C.D., Healey, J.M., and Devlin, J.F., 2005, Hydraulic tomography and high-resolution slug testing to determine hydraulic conductivity distributions: Kansas Geological Survey Open File Report #2005-36, 81 p.

### Masters Thesis

Engard, B., 2006, Estimating Aquifer Parameters From Horizontal Pulse Tests, Masters Thesis, University of Kansas, 107 pp.